İSTANBUL TECHNICAL UNIVERSITY ★ EURASIA INSTITUTE OF EARTH SCIENCES

DYNAMIC MODELLING OF BACK-ARC EXTENSION IN THE AEGEAN SEA AND WESTERN ANATOLIA

M.Sc. THESIS

Ziya MAZLUM

Department of Solid Earth Sciences

Geodynamics Programme

Thesis Advisor: Assoc. Prof. Dr. Oğuz Hakan GÖĞÜŞ

JUNE 2016

İSTANBUL TECHNICAL UNIVERSITY ★ EURASIA INSTITUTE OF EARTH SCIENCES

DYNAMIC MODELLING OF BACK-ARC EXTENSION IN THE AEGEAN SEA AND WESTERN ANATOLIA

M.Sc. THESIS

Ziya MAZLUM
(602141002)

Department of Solid Earth Sciences

Geodynamics Programme

Thesis Advisor: Assoc. Prof. Dr. Oğuz Hakan GÖĞÜŞ

JUNE 2016

<u>İSTANBUL TEKNİK ÜNİVERSİTESİ ★ AVRASYA YERBİLİMLERİ
ENSTİTÜSÜ</u>

EGE VE BATI ANADOLU'DAKİ YAY ARDI GENİŞLEMESİNİN DİNAMİK MODELLEMESİ

YÜKSEK LİSANS TEZİ

Ziya MAZLUM
(602141002)

Katı Yerbilimleri Anabilim Dalı

Jeodinamik Programı

Tez Danışmanı: Doç. Dr. Oğuz Hakan Göğüş

HAZİRAN 2016

Ziya Mazlum, a M.Sc. student of İTU Graduate School of Science Engineering and Technology student ID 602141002 successfully defended the thesis entitled "DYNAMIC MODELLING OF BACK-ARC EXTENSION IN THE AEGEAN SEA AND WESTERN ANATOLIA", which he prepared after fulfilling the requirements specified in the associated legislations, before the jury whose signatures are below.

Thesis Advisor :   **Assoc. Prof. Dr. Oğuz Hakan GÖĞÜŞ**   ....
İstanbul Technical University

Jury Members :   **Prof. Dr. Russell PYSKLYWEC**   ....
University of Toronto

Prof. Dr. Erdin Bozkurt   ....
Middle East Technical University

Date of Submission : 02 May 2016
Date of Defense   :

v

FOREWORD

This thesis was written for my master degree in Geodynamics at Istanbul Technical University, Eurasia Institute of Earth Sciences, Solid Earth Sciences Department and was supported by TUBITAK project 113Y200. In the context of this thesis, the extensional tectonics in Aegean Sea and Western Anatolia was investigated by using computer models. The model results were correlated with geological and geophysical studies in order to understand the nature of retreating subduction zones and its effects to the geodynamic evolution of the region.

I would like to thank the following people without whose help and support this thesis would not have been possible. First i like to show my gratitude to my advisor, Assoc. Prof. Oğuz Hakan Göğüş for his suggestions, motivations and approaching the different challenges during this thesis. Also my bachelor advisor Prof. Can Genç for all the scientific discussions, thoughts about the subject and encouragements. And aslo i want to show my gratitude to Prof. Russell Pysklywec for his useful comments and advises. I would like to thank Assoc. Prof. Tuna Ekinci for sharing his precious knowledge, input and help, also my project collegues Ömer Faruk Bodur Caner Memiş for their brainstorming and discussions.

Finally i would like to thank my parents Müge Kaşgöz, Mehmet Kemal Mazlum and my girlfriend Doğa Topbay for their constant support during the time i studied.

<div align="right">
Ziya MAZLUM
(Geological Engineer)
</div>

TABLE OF CONTENTS

x

SYMBOLS

LIST OF TABLES

LIST OF FIGURES

DYNAMIC MODELLING OF DYNAMIC MODELLING OF BACK-ARC EXTENSION IN THE AEGEAN SEA AND WESTERN ANATOLIA

DYNAMIC MODDELING OF BACK-ARC EXTENSION IN THE AEGEAN SEA AND WESTERN ANATOLIA

SUMMARY

The Aegean Sea/Western Anatolia back-arc has predominantly been extending due to the southward retreat of the Hellenic subduction zone. This extension has been inferrred by the widespread magmatism, detachment faulting and the exhumation of metamorphic core complexes. While there is an agreement that the active slab retreat has been producing the extension in this back-arc (since the late Oligoce-early Miocene), the real nature of this extension may also be due to the other geodynamic mechanisms (e.g post-orogenic thinning). The major objective of this thesis is to test the geodynamic evolution of the back-arc extension by using numerical modelling and reconcile the model results with the observations from the Aegean Sea and Western Anatolia.

Aegean Sea and Western Anatolia were under influence of collision between Sakarya continent and Menderes Taurides until Paleocene. The terminal closure of Northern branch of Neotethys compressed the area and it is thought that crust and lithosphere should have thickened. When the compression is worn of, the whole Aegean region started to extend. The large scale extension has been inferred by the exhumation of metamorphic core complexes (e.g., Kazdağ and Menderes massifs) and detachment faulting since late Oligocene.

Interpretations of petrological data from the volcanic units show that the first arc volcanism, associated with the Hellenic subduction zone begun at Rhodope massif during the late Oligocene, and migrated towards SW. The problem is, while the Aegean Sea has possibly extended more than western Anatolia and lowered the topography < 0, the Western Anatolia has an average 1 km elevation above sea level It is possible that the various geodynamic reconfigurations may have been effective in differing the geological evolution of these two regions. For instance, it has been suggested that the slab tear/break-off affect the Western Anatolia inferred by the seismic tomography images.

For modelling work, a geodynamic code named "SOPALE" that solves creeping flow for viscoplastic environment was used. A starting model was determined and some parameters were changed in order to understand their effects. Starting model was a simple subduction model with a thick continental lithosphere (40 km crust, 110 km mantle lithosphere) and a thinner oceanic lithosphere (100 km). The oceanic lithosphere was pushed with 1cm/year velocity in order to create a subduction. According to model results, trench was migrated 220 km to the south and crust was thinned down to 28 km. The back-arc topography was subsided 1.5 km.

In order to understand the effects of both trench retreat and breakoff, tests for continous slab retreat for Aegean Sea, and discontinous subducting slab or "tear" for Western Anatolia has been conducted. For continous slab retreat; the oceanic lithosphere thickness, density, continental lithosphere thickness and moho temperatures of the back-arc have been changed. Models with different oceanic lithosphere thickness revealed that thicker oceanic lithosphere produced more extension at the back-arc. While 70 km thick oceanic lithosphere is used, slab was retreated 180 km and crust was thinned down to 32 km. But if the lithosphere thickness is increased to 110 km, the total amount of retreat was calculated 260 km and crust was thinned down to 26.5 km. Thicker lithosphere is heavier and produces more slab pull force that required for slab retreat. Likewise models with different oceanic lithosphere densities shown that denser material increases extension at back-arc. If density of oceanic material is selected 3290 kg/m^3, the slab migrates 30 km and crustal thickness was calculated 37 km. In spite of that, if the material density is selected 3340 kg/m^3, slab retreated 200 km and crustal thickness is decreased to 30 km. The important thing here is the density difference between lithosphere and asthenosphere. Asthenosphere density was selected as 3280 kg/m^3. Bigger density difference produces more slab pull force and accordingly more extension.

One other important factor is the thickness of the back-arc lithsophere. According to models, thinner continental lithosphere supports back-arc extension. If 90 km thick continent (40 crust, 50 mantle lithosphere) is selected, slab retreat increased to 350 km and crust of the back-arc thinned down to 24 km. On the other hand, model with 130 km back-arc lithosphere (40 km crust, 90 km mantle lithosphere) indicate that amount of slab retreat decreased to 280 km and crustal thickness to 27 km. That means that the thinner back-arc lithosphere may deform easily and contributes slab retreat related extension. Previous studies indicate that lithosphere of the region may have thinned down via convective removal or delamination.

Different from Aegean Sea, experiments with discontious slabs or "tears" were conducted for Western Anatolia. To demonstrate the slab break-off, weak and dense material was used for the edge of the slab. According to tomography images, the slab is still under SW Anatolia, so break-off event has to be recent. Our models show that slab break-off is not so significant in terms of extension.

Continental lithosphere thickness seems more important to understand the geodynamic properties of the region. If Paleocene compression affected the lithosphere of Western Anatolia more than than the lithsophere of Aegean Sea, there should be an thickness difference between these two. Continental lithsophere thickness models indicate that thicker overriding plate is less likely to extend, so there should be a shear zone within the subducting slab. The tear within the slab evolved at this counterclockwise shear zone. According to this interpretation, slab tear is not a cause, its an effect. Volcanism data also show that Isparta volcanics (where the tear is found) has age of 6-4 million yeas, corresponds to tear event. Slab break-off models show the remnant of the slab still sinking beneath asthenosphere just like the tomography images.

EGE VE BATI ANADOLU'DAKİ YAYARDI GENİŞLEMESİNİN DİNAMİK MODELLEMESİ

ÖZET

Ege ve Batı Anadolu bölgesinin Helenik yitim zonunun etkisiyle genişlemekte olduğu uzun zamandır bilinmektedir. Bölge iyi çalışılmış olup, geniş alanlarda görülen magmatizma, sismik anomaliler, horst-grabenler, sıyrılma fayları ve içerdiği metamorfik kompleksler nedeniyle bir çok araştırmacının dikkatini çekmiştir. Hellenik yitim zonunun bölgedeki genişlemeden sorumlu olduğu genel olarak bilim insanları tarafından kabul edilmiş olsa da, hala devam eden bir tartışmadır. Bu probleme hem Ege Denizi hem de Batı Anadolu'nun jeodinamiğini anlamak amacıyla yapılmış sayısal modeller den elde edinlen sonuçlarla yaklaşılacaktır.

Batı Anadolu, Paleosen'e kadar Sakarya kıtası ve Menderes – Torid blokunun çarpışmasının etkisindedir. Neotetis'in kuzey kolunun tamamen kapanmasıyla bölge sıkışmaya başlamıştır, bu nedenle kabuk ve litosferin de kalınlaşmış olduğu düşünülmektedir. Sıkışmanın kesilmesi ile birlikte bölgede bir genişleme evresi başlamıştır. Bu genişleme, bölgedeki horst-grabenlere, sıyrılma faylarına ve metamorfik komplekslere bakılarak görülebilir. Kazdağ ve Menderes masiflerinde yapılan çalışmalara göre Batı Anadolu geç Oligosen' den beri genişlemektedir. Bu genişleme 3 farklı fazda gelişmiştir. İlk faz, D-B yönünde olup, Erken – Geç Miyosen boyunca sürmüştür. İkinci Geç Miyosen'de başlamış, Erken Pliyosene kadar K-G yönünde etkimeye devam etmiştir. Bir süre durakladıktan sonra 1

Bölgede Helenik yitim zonunun yay volkanizması Rodop masifinde başlamıştır. Bu magmatizmanın yaşı, güneybatıya doğru gençleşmektedir ve günümüzde Ege'nin güneyinde yer alan Santorini adasında bulunmaktadır. Bu gençleşmeye bakılarak yitim zonunun güneybatıya doğru hareket ettiğini ve bu hareketin yay ardında genişlemeye sebep olabileceği ortaya koyulmuştur. Bu bölgedeki asıl problem, eğer Ege ve Batı Anadolu genişlerken neden Ege'nin Batı Anadolu'dan daha fazla genişleyip deniz oluşturduğudur. Yapılan sismik tomografi görüntülerinden Ege Denizi'nin altında dalan levhanın tek parça olduğu, doğuda Rodos adasının altında ise kopmuş şekilde görülmektedir. Yani Batı Anadolu'nun altında dalan levhanın yırtıldığı ve yırtığın Batı Anadolu'daki genişlemeyi etkilediği düşünülmektedir.

Modelleme çalışmaları için viskoplastik malzemeler için krip hesaplamaları yapan "SOPALE" isimli kod kullanılmıştır. Bir başlangıç model oluşturulmuş ve çeşitli parametreler değiştirerek herbir parametrenin yitim zonunda meydana getirdiği etkiler gözlemlenmiştir. Bu etkiler yay ardı topoğrafyadaki değişim, göç miktarı, kabuk ve litosfer kalınlıkları olarak sıralanabilir. Başlangıç modelinde bölgenin bir çarpışma zonunda bulunması sebebiyle kalın bir kıtasal litosfer kullanılmıştır. Ortaya çıkan modelde kıtasal litosfer kalınlığı 150 km (40 km kabuk, 110 km manto litosferi), okyanusal litosfer ise 100 km olarak seçilmiştir. Okyanus malzemesi 1 cm/yıl hızla itilip yitim sağlanmıştır. Yapılan deney sonuçlarına göre yitim hendeği

25 milyon yılda geriye doğru 230 km göç etmiştir, Kabuk ise 28 km'ye incelmiştir. Yay ardı topoğrafyasının 1.5 km çöktüğü hesaplanmıştır.

Yitim göçü ve levha kırılması etkilerini görebilmek açısından Ege Denizi için kırılmamış levha, Batı Anadolu için kırılacak olan levha kullanılmıştır. Yitim göçü modellerinde okyanusal levhanın kalınlığı, yoğunluğu, yay ardının moho sıcaklığını ve kıtasal levhanın kalınlığı değiştirilmiştir. Değişik okyanusal litosfer kalınlıkları kullanılarak yapılan modeller göstermiştir ki, daha kalın okyanusal litosfer, yay ardında daha fazla genişlemeye sebep olmaktadır. Litosferin kalınlığı 70 km seçildiğinde yitim zonu 180 km göç etmekte, kabuk kalınlığı ise 32 km'ye incelmektedir. Ancak 110 km seçilirse, göç miktarı 260 km'ye çıkmakta, kabuk kalınlığı ise 26.5 km'ye düşmektedir. Bunu sebebi, kalınlıkla birlikte levhanın ağırlığı da artmaktadır. Levhanın ağırlığı, aşağıya doğru olan kuvveti arttırdığından, genişlemeyi ilk elden etkilemektedir. Benzer şekilde okyanusal litosfer yoğunlukları ile ilgili modeller, okyanus yoğunluğu arttıkça, yay ardındaki genişlemenin arttığını göstermiştir. Okyanusal malzeme yoğunluğu 3290 kg/m^3 seçildiğinde, hendek ancak 30 km göç edebilmiş, yay ardındaki kabuk kalınlığı ise 37 km'ye incelebilmiştir. Buna karşın eğer malzemenin yoğunluğu 3340 kg/m^3 seçilirse, yitim göçü 200 km'ye çıkmaktadır, kabuk ise 30 km'ye incelmektedir. Bunun sebebi, astenosfer ile litosfer arasındaki yoğunluk farkıdır. Astenosferin yoğunluğu 3280 kg/m^3 seçilmiştir. Aradaki yoğunluk farkı ne kadar büyükse, aşağı doğru olan yerçekim kuvveti o denli büyük olmakta ve yay ardında daha fazla genişlemeye sebep olmaktadır.

Bir diğer önemli faktör, yay ardındaki litosfer kalınlığıdır. Yapılan testler göstermiştir ki, eğer 90 km kalınlığında kıtasal litosfer seçilirse (40 km kabuk, 50 km manto litosferi), yitim 350 km göç etmekte, kabuk ise 24 km'ye incelmektedir. Ancak 130 km kıtasal litosfer seçilirse, yitim göçü 280 km'ye düşmekte, kabuk ise 27 km'ye incelmektedir. Bunu sebebi ince kıtasal litosferin daha kolay deforme olabilmesi ve yitim göçünü desteklemesidir. Bölgede daha önce yapılan çalışmalar, litosferin bir miktarının kaybolmuş olabileceğini göstermektedir.

Ege'den farklı olarak Batı Anadolu için levha kırılması modelleri yapılmıştır. Levha yırtılması üç boyutlu bir olay iken SOPALE kodu iki boyutta çalışmaktadır. Bu nedenle tomografi görüntüleri baz alınarak yırtılma, kırılma gibi modellenmiştir. Bunun için levha ucu daha yoğun ve deforme olarak seçilmiştir. Sismik tomografi görüntülerinde kopmuş olan levha halen GB Anadolu'da görüldüğüne göre, olayın daha yakın bir geçmişte gerçekleşmiş olması gerektiği söylenebilir. Bu nedenle modeller 7.5 milyon yıl sürdürülmüştür. Bu süre içerisinde levha 140 km göç etmiştir, kabuk kalınlığı 35 km'ye düşmüştür. Başlangıç model sonucuna göre levha göçü yaklaşık 110 km hesaplanmıştır. Sonuç olarak levha kırılmasının genişlemeye önemli bir etkisi olmadığı söylenebilir. Buradan levhanın yırtılması yada kırılmasının ortamdaki başka bir etkinin sonucu olduğu düşünülmüştür.

Litosfer kalınlığının bölgenin jeodinamiğini anlamak açısından daha önemli olduğu görülmüştür. Eğer bölgede Paleosen'deki sıkışma Batı Anadolu'nun litosferini Ege'ye oranla daha fazla sıkıştırdıysa, Batı Anadolu'nun litosferinin Ege'den kalın olduğu söylenebilir. Yapılan modellere göre kalın litosferin, ince litosfere oranla genişlemeye daha dirençli olduğu ve yitim göçünü daha az desteklediği görülmüştür. Bu nedenle okyanusal levha içerisinde bir makaslama zonu oluşmuş olabilir. Levhadaki yırtığın saat yönünün tersine yönündeki bu makaslama zonu içerisinde oluştuğu düşünülmüştür. Levha kırılması ya da yırtılması, bölgedeki genişlemenin bir sonucu olarak oluşmuştur. Yırtılmanın oluştuğu düşünülen yerde bulunan Isparta

volkanikleri, yapılan çalışmalara göre 6-4 milyon yıl yaş vermiştir. Tıpkı tomografi görüntülerindeki gibi yapılan levha kırılması modellerinde de kopmuş levha 7.5 miyon yılda astenosferin içine gömülüyor halde görülmektedir.

Anahtar Kelimeler: Ege Denizi, batı Anadolu, Genişleme Bölgesi, Dalan Levha Göçü , Levha Yırtılması, Jeodinamik, Hendek Göçü

1 INTRODUCTION

1.1 What is Lithosphere? How Lithosphere Froms?

Lithosphere is called solid, rocky shell of the Earth and extends 50 – 140 km under oceans, 40 – 280 km under continents (Pasyanos, 2010) and floats on the underlying asthenosphere (Figure 1.1). Lithosphere can be separated in to two parts: Crust and lithospheric mantle. Crust is the upmost part of the earth that we all live on. There are two type of crust. Oceanic crust is mainly composed of dark colored basalt and roughly has 7 km thick. By contrast, the continental crust has average thickness of 35 km but may exceed 70 km under some mountain regions, mainly composed of granodioritic – andesitic composition. While oceanic crust can be old as 180 million years and has average 3 g/cm^3 density, continental crust has only 2.7 g/cm^3 density and can be 4 billion years old.
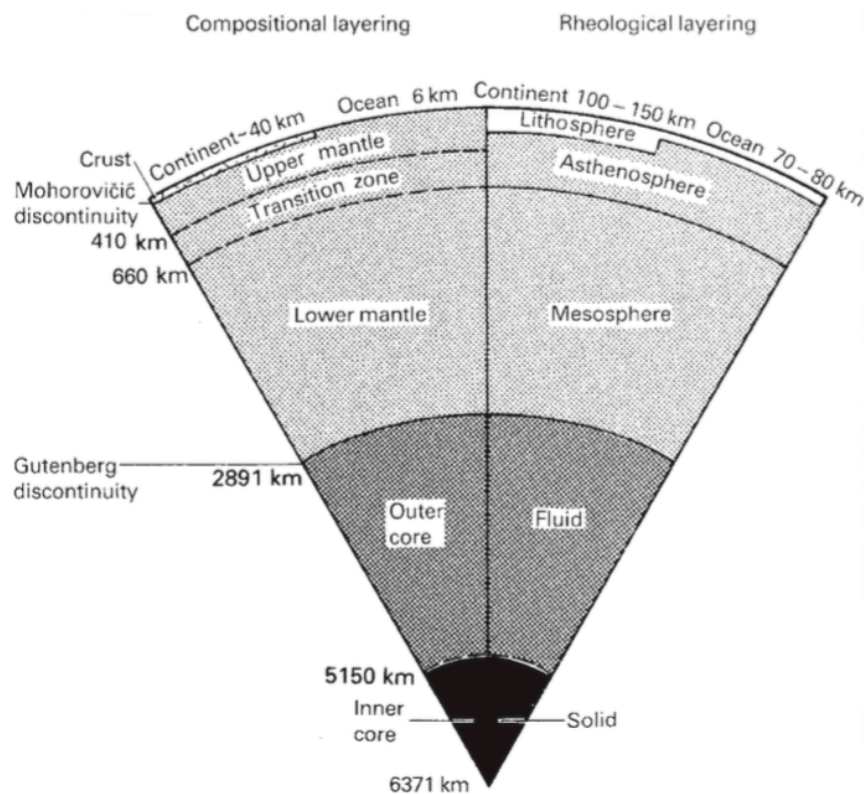
Figure 1.1 : Comparison of the compositional and rheological layering of the Earth.

Just like the crust, there are two types of lithosphere; oceanic and continental. Mid-ocean ridges are divergent plate boundaries and produce the oceanic lithosphere. The ocean lithosphere thickens and gets denser away from the ridge. Dense oceanic lithosphere tends to subduct beneath less dense continental lithosphere at subduction zone. This zone operates as a recycling system of the Earth and allows creation of continental lithosphere. The subducted oceanic material carries water to the asthenosphere. The hydration of the asthenosphere lowers the melting point of the felsic material. Melted material forms felsic volcanic and plutonic rocks (arc magmatism). This process is called partial melting.
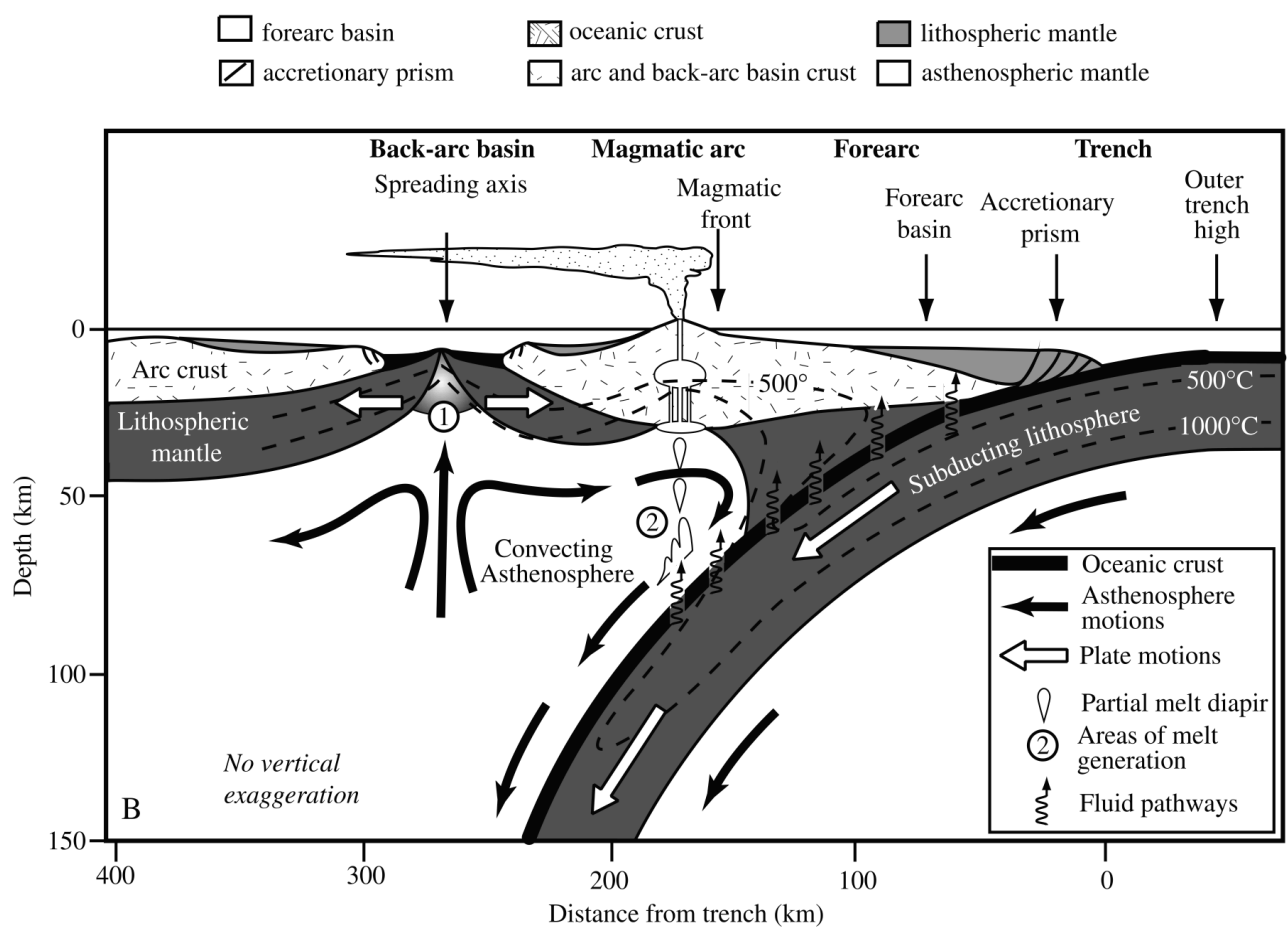
Figure 1.2 : The detailed figure of a subduction zone (From Stern, 2002).

Moho discontinuity separates crust and underlying lithospheric mantle and represents seismic wave velocity change. Above Moho, P-wave velocity is around 6.7-7.2 km/s. On the other hand, P-wave velocity increases to 7.6-8.6 km/s below Moho. This boundary represents the composition change of basaltic to ultramafic (Mantle Rocks). Beneath it, mantle lithosphere begins. Lithospheric mantle mainly consists of

2

peridotites like dunite and harzburgite. The boundary between lithosphere and asthenosphere is called lithosphere-asthenosphere boundary (LAB) and has average $1350^{0}C$ temperature. Even lithosphere is not homogenous within itself. Deeper parts of the lithosphere with increasing temperature and pressure (geoterm), the behavior and rheology of the material differs. This variations were detected by geophysical studies and measurements. Seismic wave velocity within lithosphere is a function of density.

Asthenosphere may be considered as the viscous part of the mantle and mainly composed of olivine. Asthenosphere basically flows because of its temperature. Deeper parts of the world will get hotter and heated material starts to move upwards. By the same time, colder material tends to sink. This phenomenon is called "mantle convection". Scientists measured asthenospheric viscosity by using post-glacial rebound theory. According to this event, 3 km thick ice sheet at last glacial maximum (20.000 years ago) was melted down and pressure relaxation caused the land uplifted. By using this uplift rate, the viscosity of the asthenosphere has been measured 10^{-21} Pa for 120 – 670 km depth (Peltier, 1986).

Asthenospheric mantle exceeds up to 410 km depth. At this region, with increasing temperature and pressure, atoms within the olivine crystals are rearranged and form wadsleyite mineral. This transition increases density of the material. At roughly 660 km depth, transition zone ends and mesosphere begins. This boundary is called 660 km discontinuity and was formed because of phase transition of olivine minerals at certain depth and temperature. Olivine minerals are transformed into perovskite at 660 km depth which density is dramatically increases. Below that layer, mesosphere begins but within this thesis, deeper parts of the Earth was not interested.

1.2 Slab Rollback Process and Retreating Trenches

A subduction system may be divided into 4 regions while considering its surficial properties: Trench, forearc, magmatic arc and back-arc (Figure 1.2). Trench is the region where oceanic lithosphere subducts under overriding plate. Trenches may represent themselves as deep pockets like Mariana Trench, deepest part of the Earth. Behind the volcanic arc, back-arc is formed. There are two types of back-arc according to its surficial properties: 1) Compressional back-arc (Chilean Type), 2) Extensional back-arc (Mariana Type).
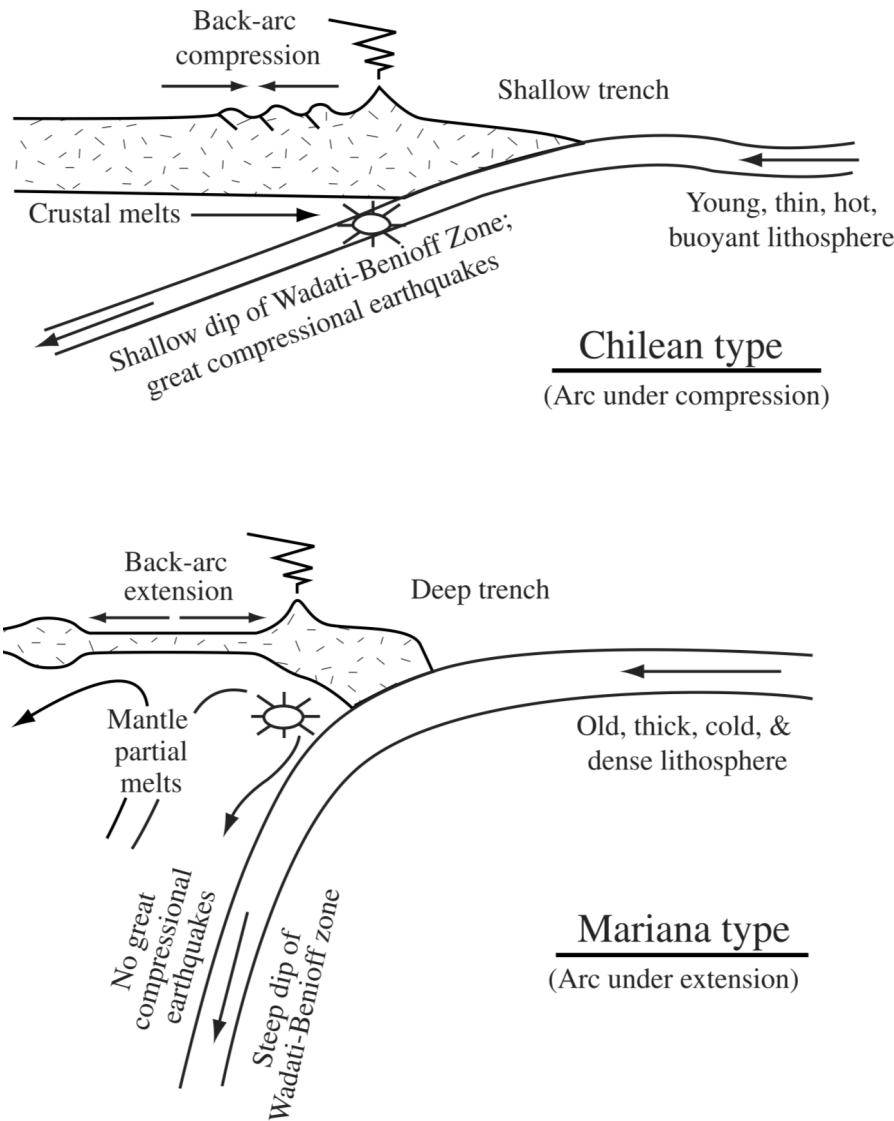
Figure 1.3 : Types of Subduction Zones (Uyeda & Kanamori, 1979).

If the subducting lithosphere is young, hot and thin; cannot easily subduct because of its high buoyancy. The slab sinks into asthosphere with relatively low angle and trench starts to migrate towards continent. The subducting plate compresses the arc structure, creates compressional back arcs. This type of back-arc represents high topography like Andes or Himalaya. But if the lithosphere is old, thick and cold, it has low buoyancy and tend to sink (Uyeda & Kanamori, 1979) (Figure 1.3). Subducting lithosphere steepens and slab pull force increases. Trench starts to migrate towards incoming plate and back-arc extends. This phenomenon is called trench migration or slab rollback. If the lithosphere is overextended at back-arc, rifting or even sea floor spreading may begin (Jarrard,1986). Trench retreat related extensional back-arcs were investigated during this thesis.

4

1.3 Basics of Rheology

Rheology interests with deformation and flow of materials under influence of an applied stress (Ranalli, 1995). In order to understand the rheology of the Earth; stress, strain, strain rate and strength should be defined. Stress is force per unit area and may expressed as kilograms per square meters.

The deformation on materials may be recoverable or unrecoverable. Recoverable deformation means when the stress is removed, the material should return to its initial shape and the strain should be zero. But if the deformation is unrecoverable, the material cannot return to its initial shape when stress is removed. The deformation type could be faulting or folding. If stress is applied to a material, its original volume or shape may be changed. This is used to define the deformation or strain of the material. If the strain is time dependent, it represents the strain rate. The strength of a material is described as the maximum stress that the material resists the deformation.

There are 4 types of material behaviors: 1) Brittle; 2) Elastic; 3)Visco-elastic and 4) Viscous.

Deformation of Materials

In geology, pressure is generated by crust or lithosphere itself. The lithostatic pressure and tempreature increase with respect to depth. This pressure and temperature change the behavior of the material and determine its deformation type. In the shallow depths in crust, if the imposed pressure is removed, material comes back to its original shape and volume. This deformation type is called brittle deformation.

When the magnitude of stress elapses the strength of the material, it causes progressive failure network of various scaled cracks. These cracks closes under compression deep within the crust, and completely terminated near 5 km depth. Also materials compressive strength is much greater that the tensile strength. For example, compressive strength of granite is 140 MPa, and its tensile strength is only about 4 MPa.

Experiments show that materials tend to fracture at angles of 45^0 when a critical shear stress is exceeded. According to Mohr-Coulomb fracture criterion this critical shear stress is defined by;

$$|\sigma_s^*| = c + \mu\sigma_n$$

Where, σ_s^*; critical shear stress, σ_n; normal stress, μ; internal angle of friction and c; cohesion. Cohesion is the shear resistance of a rock under zero normal stress. The strength of rock increases by the pressure of the surrounding neighbor rocks. This confining pressure inreases with depth, until 10 -15 km. Below that point, temperature takes the effect, and material starts to weaken. But this relationship is complicated because of fluid content, rock composition and preexisting weaknesses.

On the other hand, at certain point deeper into the Earth, the material starts to creep. This type of deformation is permanent and is called ductile (plastic) deformation. Ductile flow is dependent upon temperature and pressure. Increasing temperature will speed up the strain rate, while increasing pressure produces more pompous flow. The governing equations about plastic and visco-plastic flow will be given at section 2.1.
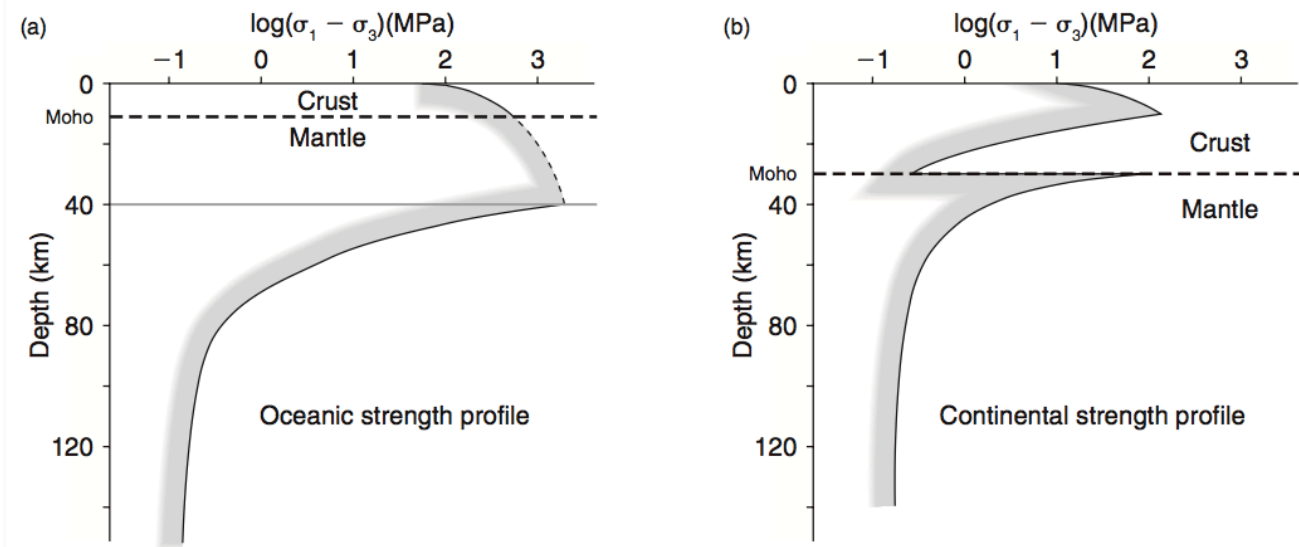
Figure 1.4 : Strength profiles for a) Oceanic; b) Continental lithospheres.

1.1 Literature Review

Aegean Sea – Western Anatolia back-arc is under influence of N – S extension since Late Oligocene – Early Miocene. It was claimed that Menderes core compex that exhumed at Upper Miocene was cut by E-W trending grabens (e.g Gediz, Alaşehir, Büyük Menderes, Küçük Menderes) (Bozkurt & Sözbilir, 2004). The border between grabens and metamorphic massif is defined as low dipping (15^0) detachment faults. (Emre & Sözbilir, 1997; Bozkurt & Sözbilir, 2004; Yılmaz et al., 2000, Çemen et al., 2006). Menderes Massif is limited by İzmir – Ankara - Erzincan suture zone and represents the continent collision between Menderes block and Sakarya continent at Late Paleocene (Şengör & Yılmaz, 1981; Seyitoğlu et al., 1996). After this collision, the northern branch of Neotethys was terminally closed, Western Anatolia get compressed since Eocene and lithosphere was thickened.

1.1.1 Volcanism Data

The region is characterized by widespread volcanism. This volcanism can be separated as subduction - related and asthenospheric sourced magmatism. The late Oligocene and younger calc-alkaline volcanics are considered as subduction related (Fytikas et al., 1984; Pe-Piper & Piper, 1989, 2002, 2006, 2007) (Figure 1.5). If the age of subduction related volcanism is tracked, it can be seen that ages are getting younger closer to the trench. First island arc magmatism that was generated by Hellenic subduction zone was is exposed at the Rhodope Massif in the north (Marchev et al., 2005) then was migrated towards S-SW. Some researchers think that same magmatism continues today near Southern Aegean Volcanic Arc (Pe-Piper & Piper, 1989, 2002). If the arc magmatism is migrating towards southwest, the subducting African lithosphere must migrate as well (Dewey ve Şengör, 1979; McKenzie, 1975; Meulenkamp et al., 1988).

The second type of volcanism is interpreted as Early Miocene asthenosphere - sourced alkaline magmatism (Aldanmaz et al., 2000) and may have been produced by convective removal (Dilek & Altunkaynak, 2009). Specifically, this removal may be interpreted as lithospheric loss or thinning beneath Western Anatolia (Aldanmaz et al., 2000) or even Aegean Sea.
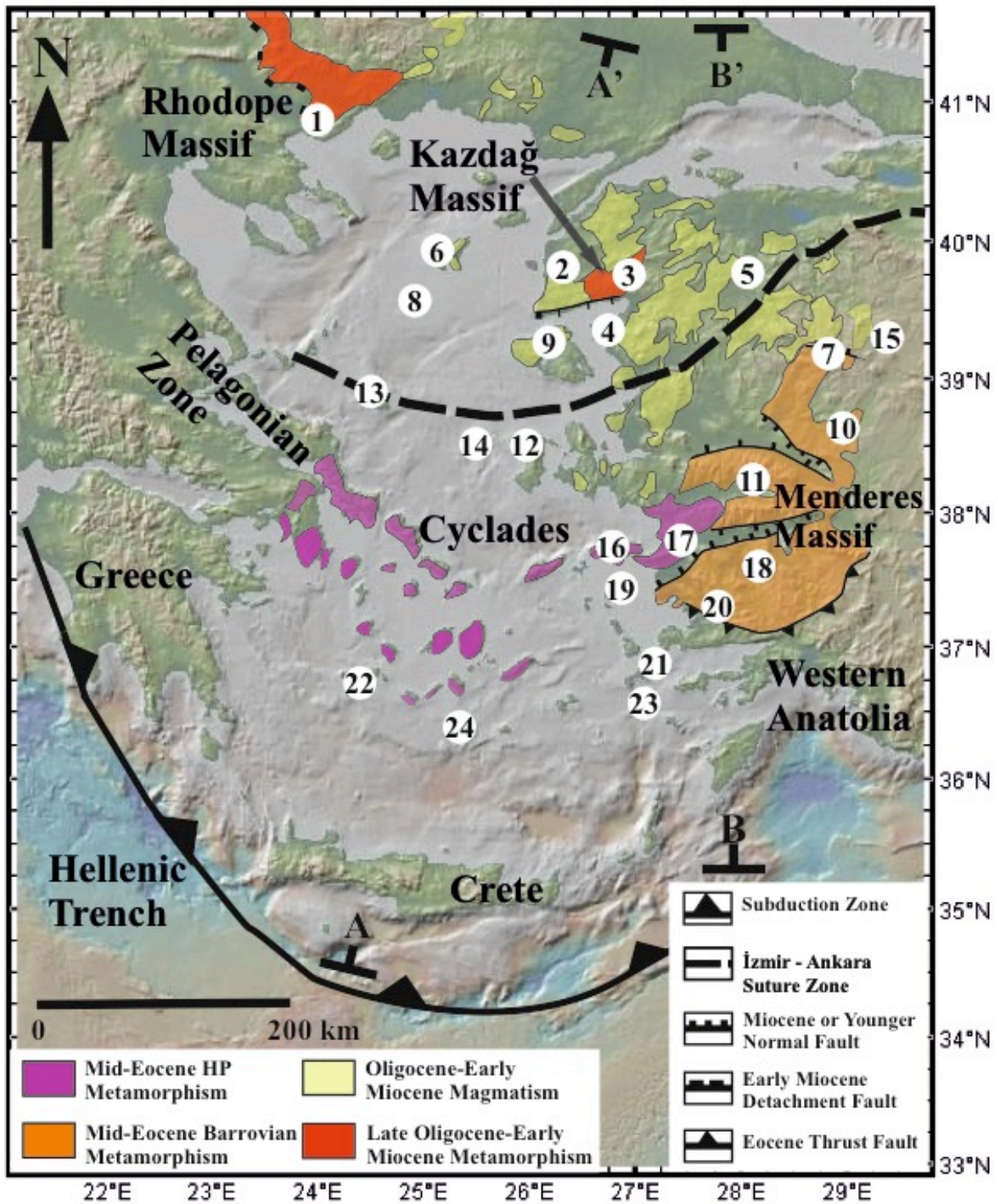
Figure 1.5 : A) Tectonic map of the region. Numbers in white circles corresponds to volcanic units (See Figure 1.6). A-A' and B-B' are the crossections of seismic tomography of Van Hinsbergen et al., (2010).
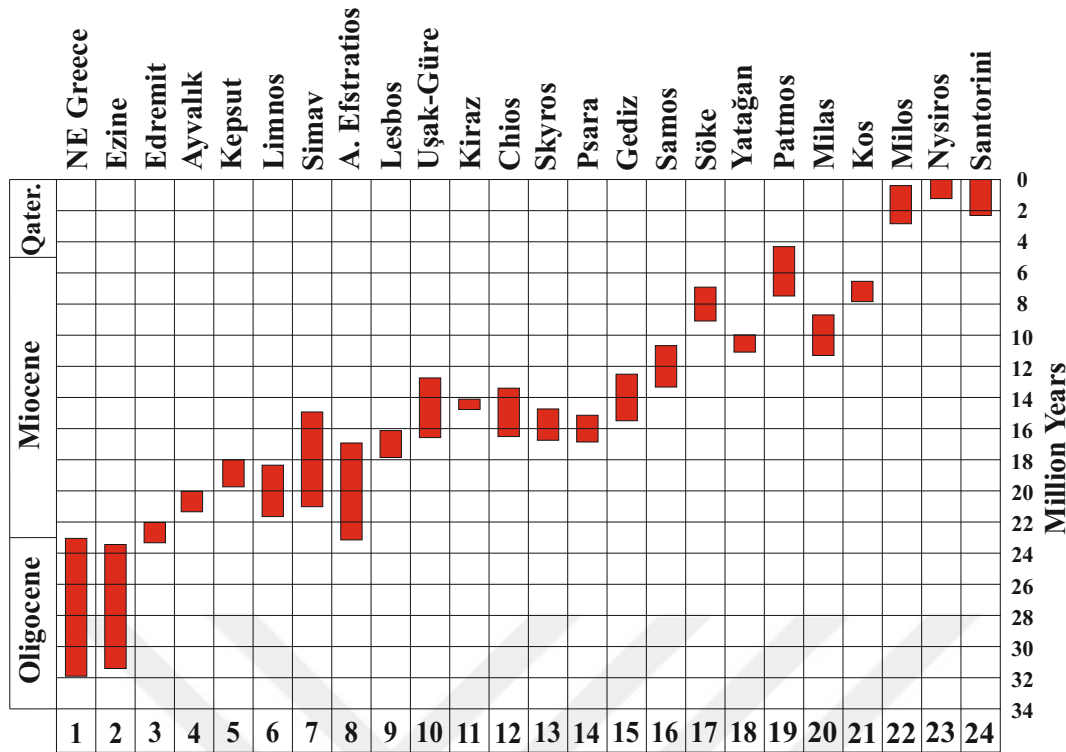
Figure 1.6 : Ages of volcanic units within the map (See Figure 1.5) (Data from Seyitoğlu & Scott, 1992; Bozkurt et al., 2008; Ercan et al., 1985, 1995; Pe-Piper et al., 1994, 2009; Çoban et al., 2012; Fytikas et al., 1979, 1984; Innocenti et al., 2005; Pe-Piper & Piper, 2013; Karaoğlu et al., 2010; Emre & Sözbilir, 2005; Pe-Piper, 1995).

1.1.1 Lithosphere Stucture

The seismic tomography studies along Aegean Sea and Western Anatolia indicates that the high velocity zone found at south of Crete is the retreating ocean slab that may responsible for the extension of the Aegean sea and Western Anatolia (e.g Biryol et al., 2011, Meulenkamp et al., 1988, Taymaz et al., 1990, Wortel & Spakman, 2000, Piromallo & Morelli, 2003). Tomography images also show that the African oceanic lithosphere subducts under Aegean sea with 50^0 dipping angle and reaches out 660 km depth (Asthenosphere – Mesosphere boundary) (Edwards & Grasemann, 2009). The ocean slab beneath Aegean Sea seems like continuous, but discontinous beneath Western Anatolia. This discontinuity indicates slab break-off or slab tear within the African lithosphere (Van Hinsbergen et al., 2010). Seismic tomography studies also points out the low velocity zones beneath crust and these zones may correspond to hot asthenosphere penetrated near the crust (Van Hinsbergen et al. 2010; Biryol et al. 2011; Kömeç-Mutlu & Karabulut, 2012; Salaün

10

et al, 2012). The lithosphere thickness is around 100 km beneath Western Anatolia according to P and S wave velocity measurements of Sodoudi et al., (2006). The same study indicates that the Aegean crustal thickness is between 21 – 27 km. The crustal thickness measurements at Western Anatolia show around 25 km thick (Karabulut, 2013).

Although Aegean Sea and Western Anatolia are pieces of the same geodynamic system, it was claimed that they have different geological properties. While the average topography at Western Anatolia is around 1 km, Aegean region is under water. The geodynamic system that uplifts the Western Anatolia and subsides Aegean sea is still not well known.

1.2 Hypothesis

By using the geological, petrological, and seismic data mentioned above, three models were proposed for the main triggering mechanism of the extension. First one is the westward escape of Anatolian plate. That model was proposed by Dewey & Şengör (1979) and speculates that the collision between Arabian platform and Anatolia compressed the Eastern Anatolia and transferred the stress to the west because Eurasia behaves like craton. This stress transfer caused extension at Aegean Sea and Western Anatolia. Recent studies show that collision between Arabian platform and Anatolia is around 15 million years (Okay et al., 2010), but there are basins that was formed at Oligocene in Western Anatolia. So this model is not valid in the view of this information.

Another alternate model is the gravitational collapse. Seyitoğlu & Scott (1996) suggests that the extension in Western Anatolia began 20 million years ago and this extension is too early to be explained by western escape model (Dewey & Şengör, 1979) or retreating Aegean trench (Le Pichon & Angelier, 1981). The lithosphere is thickened up to 55 km because of the collision (Şengör, 1985) and tend to collapse under its own weight. Consequently, the compression was fade off at Paleocene and overthickened lithosphere was collapsed and triggered the extension at Aegean Sea and Western Anatolia (Seyitoğlu & Scott, 1996).

The third hypothesis is the extension triggered by retreating Hellenic trench. It is known that the convergence velocity between Afica and Eurasia is not stable (Jolivet

& Brun, 2010). Jolivet & Faccenna (2000) claim that the convergence velocity between Africa and Eurasia decreased, compression in Western Anatolia was diminished. Then triggered the slab retreat and started the extension in the region. First volcanic material produced by Hellenic arc was found at Rhodope massif (Marchev et al., 2005). The subduction related arc volcanism is getting younger towards the south and active arc can be found at Santorini island (Pe Piper & Piper; 2002, 2006, 2007). So the trench should have migrated to south. The studies at Kazdağ Massif indicates that Late Oligocene – Early Miocene metamorphic complex was cut down by a granitic pluton, exhumed along a shear zone (Okay & Satır, 2000). In the same study, it was speculated that this kind of extension may only be produced by the retreating trench at Hellenic subduction zone because there was no evidence of high topography in order to support the gravitational collapse. Also Bozkurt & Oberhansli (2001) claim that Menderes Massif was started to exhume 20 million years ago. So it can be interpreted that he extension may have propogated from north to south.

As it was mentioned above, the most suitable mechanism explaining the extension of Aegean sea and Western Anatolia is the slab retreat hypothesis. Numerical models were produced in order to understand the retreat mechanism and its effect to back-arc area.

2   METHOD AND MODEL SETUP

2.1   Numerical code and governing equations

The subduction retreat experiments in this thesis were conducted with the SOPALE geodynamic modeling numerical code. This code utilizes both Eularian and Lagrangian gridding systems to operate and uses arbitrary finite element method to solve creep deformation of incompressible visco-plastic materials (Fullsack, 1995). The governing equations are conservation of mass, momentum and energy;

$$\nabla \cdot u = 0$$

$$\nabla P + \nabla \cdot \sigma' + \rho g = 0$$

$$\partial T / \partial t = k \nabla^2 T + H$$

Density is a function of temperature,

$$\rho(T) = \rho_0 (1 - \alpha (T_1 - T_0))$$

ρ, u, P and T represent the fields of density, velocity, pressure and temperature; g, k, H and t are gravitational acceleration, thermal conductivity, radioactive heat production (per unit mass) and time.

$$\sigma' = \min \{\sigma_v; \sigma_y\}$$

Plastic yield stress is defined by (Coulomb criteria),

$$\sigma_y = P \sin \phi + c_c \text{ (For crust)}$$

$$\sigma_y = c_m \text{ (For mantle)}$$

The viscous stress is defined by,

$$\sigma_v = 2\,\eta_e\,\dot{\epsilon}$$

For rheological calculations laboratory measurements based on a viscous flow law of $\dot{\varepsilon} = A\sigma^n \exp(\dfrac{-Q}{RT})$. Here, $\dot{\varepsilon}$ is the strain rate, T is temperature, σ is deviatoric stress, and the variables A, n, Q and R are the viscosity parameter, power law exponent, activation energy, and ideal gas constant, respectively. For continental crust A= 1.1 x 10^{-4} MPa^{-4}/s, n = 4, and Q = 223 kJ/mol are used, based on wet quartzite (Gleason and Tullis, 1995). The variables A, n and Q are the viscosity parameter, power exponent and activation energy (from laboratory experiments) and R is ideal gas constant.

2.2   Material Parameters and Boundary Conditions

The configuration of the model (Figure 2.1) is designed as a general representation for the retreating subduction of the oceanic lithosphere (pro-plate) under continental plate (retro-plate) at the plate boundary region where the subducting slab is physically available for driving slab retreat/roll-back. Numerical experiments are conducted within the solution box 2000 (width) x 660 (height). The bottom of the solution box corresponds to upper-lower mantle phase transition boundary where such transitory effects are not considered. The width of the solution box, 2000 km sufficient to to consider the small-scale convection effects in the mediterranean orogen (Faccenna and Becker, 2010).

1 cm/year velocity was imposed from upper right side of the box in order to create subduction due to predictions of Jolivet & Faccenna (2000). Upper left side of the solution box is fixed (Anatolian microplate cannot move northward). The same amount of material entered from upper right side of the solution box (ocean subduction) is conducted away from the asthenospheric part of the lithosphere simetrically in order to balance the mass.
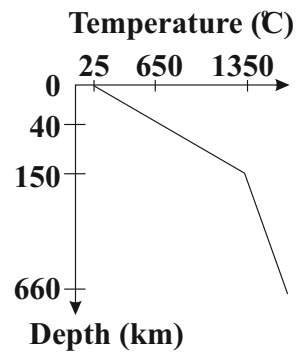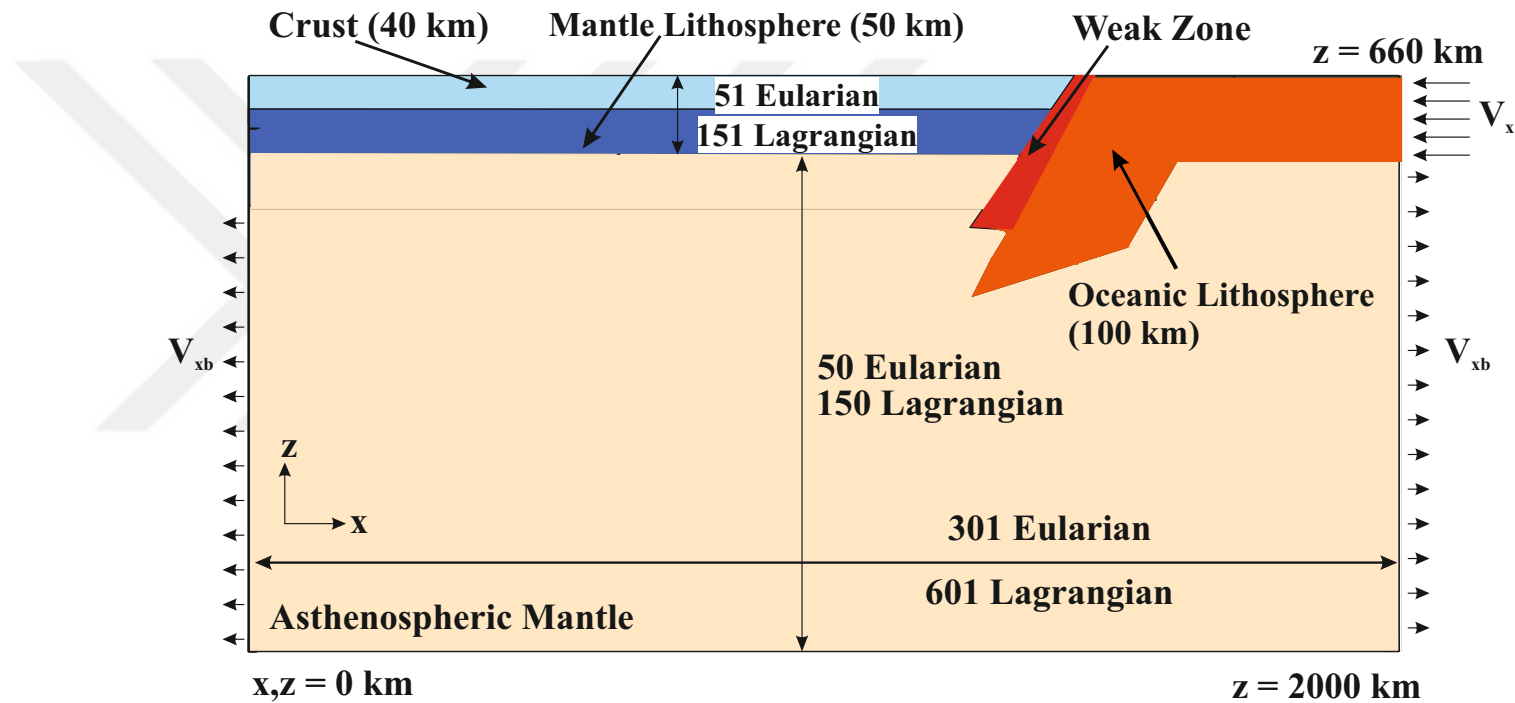
Starting model (RET-1) has 40 km thick quartzite crust, 50 km thick olivine continental mantle lithosphere and 100 km thick olivine oceanic lithosphere (Fig.2.1). A weak zone was put between the oceanic and continental lithospheres to allow localized deformation between the plates.

Table 2.1 : Reference for viscosity parameters: For continental mantle lithosphere, wet olivine; oceanic mantle lithosphere and asthenospheric mantle, dry olivine (Hirth & Kohlstedt, 1996), and for crust, wet quartzite (Gleason & Tullis, 1995).

	Parameter	Continental Crust	Continental Mantle Lithosphere	Asthenospheric Mantle	Oceanic Mantle Lithosphere
A	Viscosity Parameter	1.1×10^{28} Pa^{-4}/s	5.49×10^{25} Pa$^{-4.48}$/s	5.49×10^{25} Pa$^{-4.48}$/s	5.49×10^{25} Pa$^{-4.48}$/s
n	Power Exponent	4.0	4.48	4.48	4.48
Q	Activation Energy	223 kJ/mol	498 kJ/mol	498 kJ/mol	498 kJ/mol
Φ	Internal Angle of Friction	15^0	15^0	15^0	15^0
ρ_0	Density	2800 kg/m^3	3300 kg/m^3	3280 kg/m^3	3350 kg/m^3
σ_y	Plasticity	1 MPa	100 Mpa	0 Mpa	100 Mpa
α	Coefficient of Thermal Expansion	2.25×10^{-5} K^{-1}	2.25×10^{-5} K^{-1}	2.25×10^{-5} K^{-1}	2.25×10^{-5} K^{-1}

Continental and oceanic mantle lithosphere thickness, convergence velocity, density and Moho temperature parameters were changed to calculate the amount of deformation (maximum subsidence, minimum crustal and lithsopheric thicknesses) at the back-arc area and trench retreat. Also some tests with uniform lithosphere thickness were conducted in order to correlate with other models. It was assumed that there is a continous slab beneath Aegean Sea and discontious slab under Western Anatolia (Van Hinsbergen et al., 2010). So, the slab tear or break-off models were prepared for Western Anatolia.

Figure 2.1 : Model Setup of RET-1 (Starting Model). Below, temperature gradient and materials physical properties were given.

3 TRENCH RETREAT RELATED BACK-ARC EXTENSION MODEL RESULTS

The RET-1 model configuration starts with ocean lithosphere subduction under the continental lithosphere at the plate boundary (e.g trench position at t = 2.5 Myrs) (Figure 3.1). The amount of slab retreat is at the early stages of the model where a portion of the slab is subducting vigorously under such plate boundary (Stage 1). We note that the amount of slab retreat is 110 km until t = 2.5 Myrs and the crust is thinned 4 km, corresponding to 0.5 km of maximum subsidence in the continental back-arc. Following to this stage, ocean lithosphere subduction develops in relatively rapid and continous pace until the ocean slab hits the bottom of the solution box (t = 13.5 Myrs) (Stage 2). This relatively constant period of subduction until the slab's hit is apparent from the model graphs in which the pace of retreat, crustal thinning decrease afterwards. By t = 13.5 Myrs, the amount of retreat is nearly 310 km and the crust is thinned 13 km compared to t = 0. Such decrease in the pace of the subduction and the retreat continues until t = 21 Myrs while the slab is not moving in after reaching the steady state conditions (Stage-3). From then on between t = 21-25.5 Myrs (Stage 4), the pace of subduction increases again until t = 25.5 Myrs similar to stage 2. This is most likely because the heavy slab in the subduction system has reached critical length and weight when the slab has ability to retreat (roll back) near the edge of the solution box. The continental material carried down by ablative subduction was reached 560 km depth within the asthenosphere in t = 25.5 Myrs.
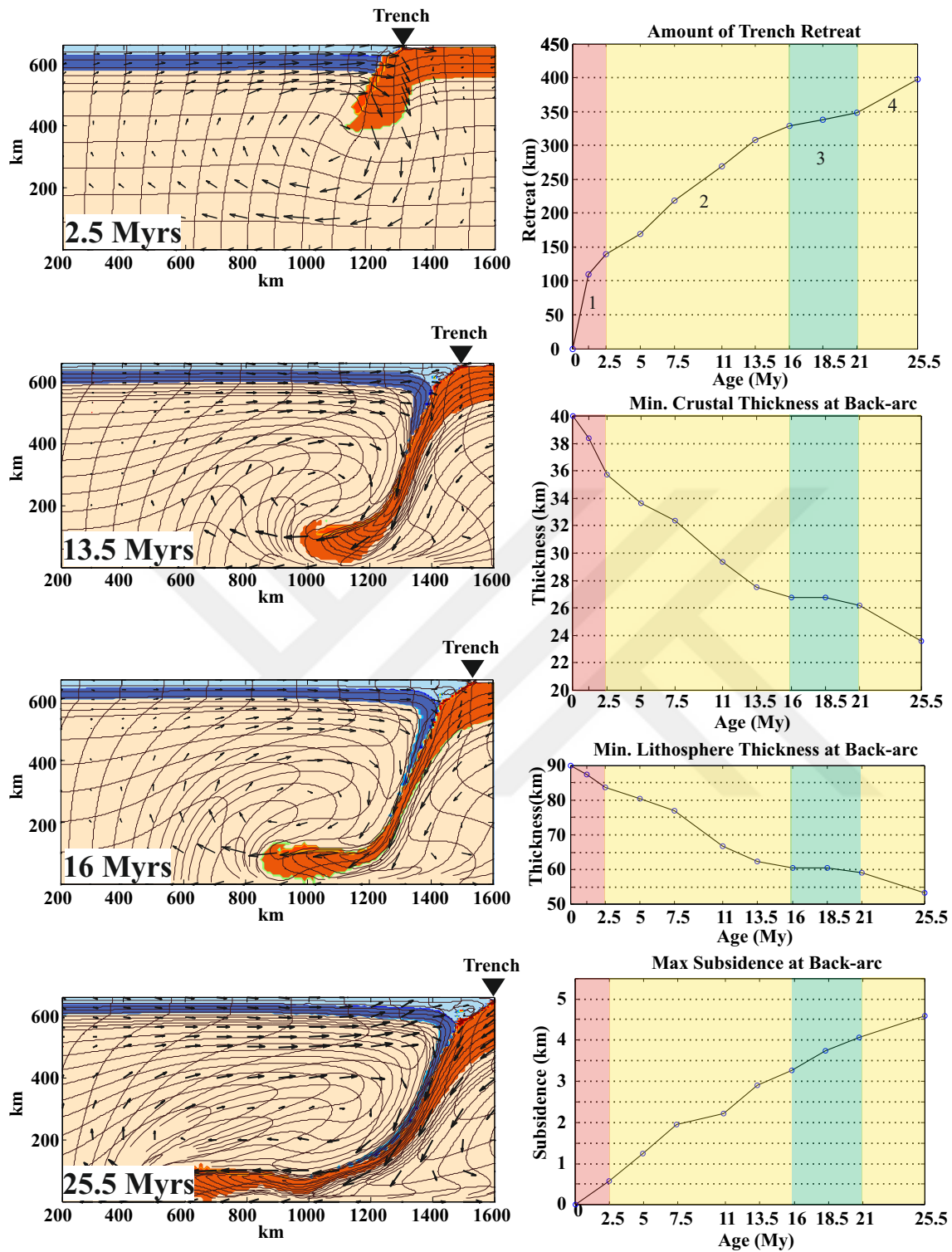
Figure 3.1 : Model Results for RET-1.

3.1   The Effect of Continental Lithosphere Thickness

At this set of models, the effect of continental lithosphere thickness was investigated. Aegean Sea and Western Anatolia regions are characterized by Paleocene compression and thickening. Due to this reason, conducting different experiments with various lithosphere thickness may be useful for understanding the nature of the retreating slabs. The starting model (RET-1) has 90 km continental lithosphere thickness (40 km crust, 50 km lithospheric mantle), experiments with 110 km (40 km crust, 70 km lithospheric mantle) (RET-2), 130 km (40 km crust, 90 km lithospheric mantle) (RET-3) and 150 km (40 km crust, 110 km lithospheric mantle) (RET-4) were performed. To understand its effect, other parameters kept same as RET-1.

The result of RET-1 was correlated with thinner lithospheres. In RET-3 (90 km lithospheric mantle thickness), after t = 1.25 Myrs trench retreat quickly increases. At t=18.5 Myrs, ocean lithosphere is thinned down 280% of its original thickness at 360 km depth. The lying part of the ocean lithosphere increases with thinner continental lithosphere thickness. The thinner overriding plate enables ocean lithosphere to subduct effortless due to lesser frictional force between plates. Oceanic lithosphere easily deforms continental lithosphere because continental lithosphere loses strength while thining. At RET-2 test (thinner continental lithosphere) trench retreat reached 350 km and max. subsidence, 4.1 km. Crustal thickness is thinned down to 24 km. Continental material is dragged down 560 km depth within the asthenosphere and to the forearc area. The crust in front of the trench is thickened about 100 km. By t = 25.5 Myrs, the back-arc crust and mantle lithosphere have similar thickness.

Table 3.2. Model Results of continental lithosphere thickness tests

Model	Retreat	Max. Sub	Cru.Thick	Lith. Thick	β factor
RET-2	320 km	2.9 km	25.75 km	72 km	1.55
RET-3	280 km	2.4 km	27 km	90 km	1.48
RET-4	220 km	2.3 km	28.25 km	110 km	1.41
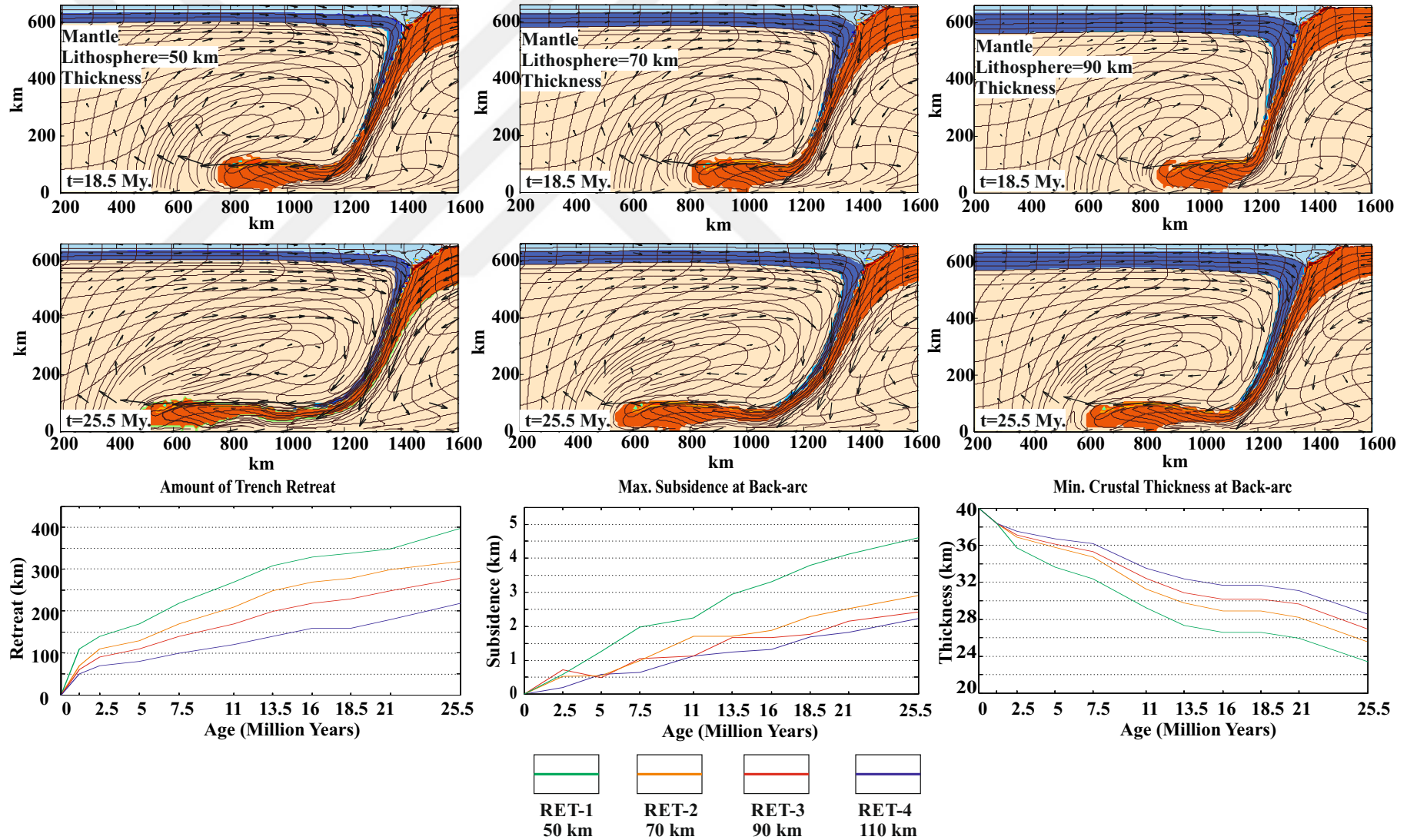
Figure 3.2 : Effect of back-arc lithosphere thickness. Model with 90 km (Left), 110 km (Middle) and 130 km (Right) thicknesses. Amount of extension decreases with back-arc lithosphere thickness.

3.2 The Effect of Subducting Ocean Lithosphere Thickness

At this set of models, the role of the ocean lithosphere thickness on the slab retreat and the resulting back-arc extension is investigated. Previous studies in the mediterranean region suggests that the ocean lithosphere thickness can vary from 70 to 110 km . Recent study suggests that the LAB in the Ionian ocean plate-70 km (Agosinetti, 2015) and in the Aegean subduction system this can reach up to 110 km (Sodoudi et al., 2006). To further understand the effect of ocean lithosphere thickness was changed and all other parameters kept same with respect to the initial model (RET-1). Lithospheric thickness depends on the distance where lithosphere was created. At mid-ocean ridges, this thickness is "0 km" and the lithosphere thickness away from the ridge (Stein and Stein, 1992).

Starting from this point of view, different oceanic lithosphere thicknesses are tested to demonstrate how it will affect the slab retreat. Starting model has 100 km subducting slab thickness; experiments with 70 (RET-5) , 80 (RET-6) and 120 km (RET-7) were performed.

The results of the RET -1 (initial model) is compared against the models with thicker ocean lithosphere thickness and the thinner ones. In RET-2, with 110 km thick ocean lithosphere, the geodynamic evolution of the model is similar to the RET-1, since the ocean subduction develops faster in the first 1.25 Myrs and then the velocity of the subduction retreat decreases but still persistent until the end of the experiment. The overall amount of subduction retreat is nearly 50 km between RET-1 and RET-2 and this amount does not change much since t = 11 Myrs. Such difference between the amount of retreat reflects on to the change between the maximum crustal thinning/extension in the back arc region. If slab is thicker, it will have more weight and has more power to deform the overriding plate.

The models with thinner oceanic lithosphere (RET-3-4-5) shows lesser amounts of slab retreat in respect to RET-1. The amount of retreat systematicly increases with depth and evolves similarly until 13.5 Myrs. The total amount of retreat at these three thinner oceanic lithosphere thinkness models are closer to RET-1 then RET-2; so it can be considered that 100 km thick oceanic lithosphere is critical value for retreat dynamics. By t=16 Myrs, the slabs are nearly at the bottom of the box and

significantly streched, even slab at RET-3 is broken-off. Namely, dense and thin ocean lithosphere can not lift its weigth and may break-off.

Table 3.1. Model Results of oceanic lithosphere thickness tests.

Model	Retreat	Max. Sub	Cru. Thick	Lith. Thick	β factor
RET-5	315 km	2.4 km	28 km	63 km	1.42
RET-6	325 km	2.6 km	26.5 km	60 km	1.50
RET-7	370 km	4.1 km	23.5 km	53 km	1.70
RET-8	430 km	4.4 km	22 km	50 km	1.81
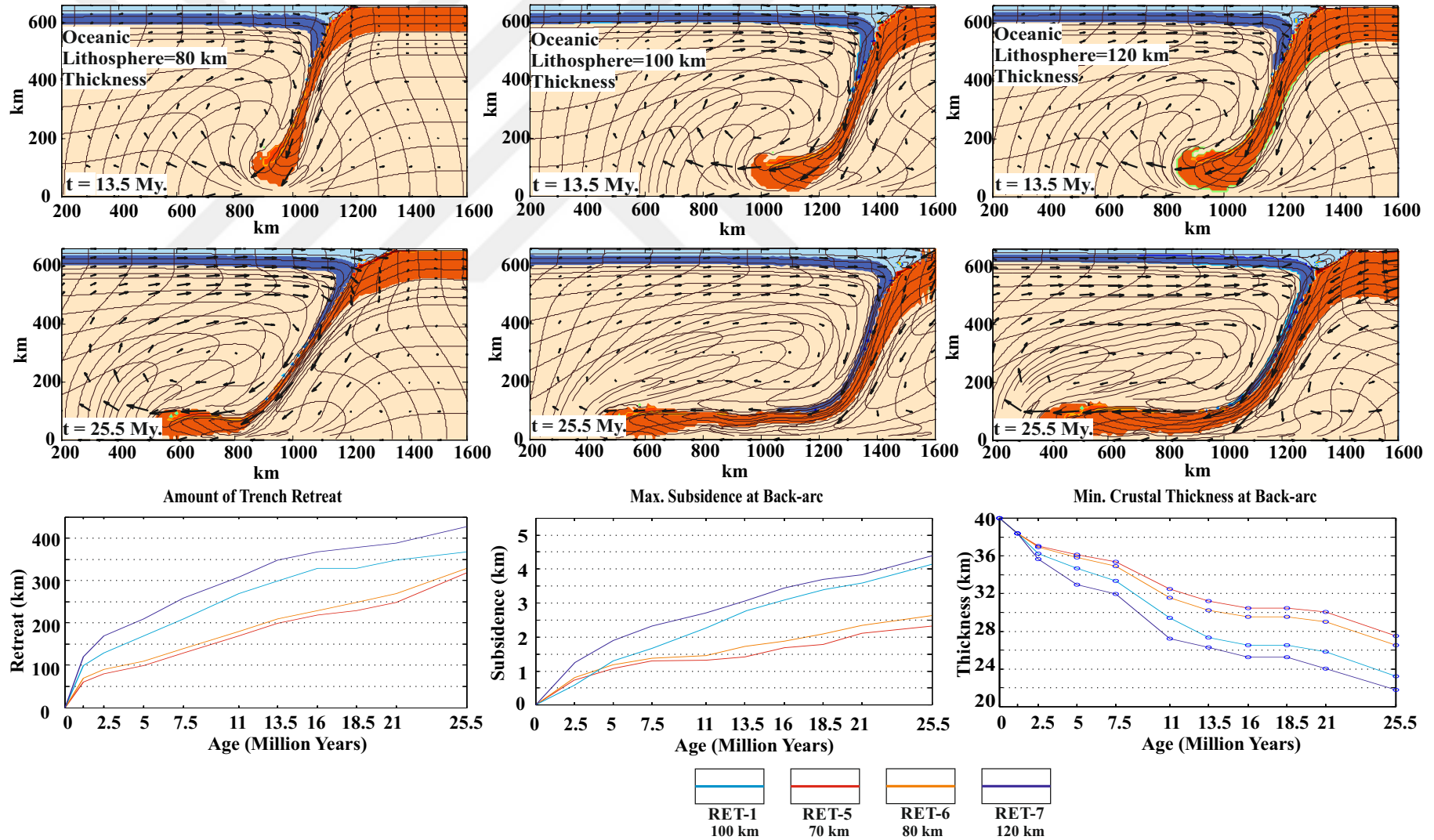
Figure 3.3 : Effect of oceanic lithosphere thickness. Model with 70 km (Left), 90 km (Middle) and 110 km (Right) thicknesses. Amount of extension increases with oceanic lithosphere thickness.

3.3   The Effect of Subducting Slab Density

It is well known that the oceanic slabs gets denser when they get old. Therefore it is thougt that density is the key component for slab retreat. For example Chilean type slabs advance because of young, less dense oceanic material (Buoyant) but Mariana type slabs retreat because of old and dense oceanic material (Uyeda & Kanamori, 1979). In order to understand its effect, the density of the subducting ocean slab was changed between 3290 and 3350 kg/m^3 (Fig.8).

Starting model has 3350 kg/m^3 slab density, so models with 3290 (RET-9), 3300 (RET-10), 3310 (RET-11), 3320 (RET-12), 3330 (RET-13), 3340 kg/m^3 (RET-14) and 3360 (RET-15) slab densities were tested and compared with RET-1 (3350 kg/m^3) and among each other. By looking the graphs at Figure 3.5, one can say that ocean slab density has significant role at retreating trenches. At RET-9 and RET-10 experiments (Low density), it can be seen that density difference between subducting ocean lithosphere and asthenosphere is too small, the slab cannot even sink into asthenosphere. By t = 25.5 Myrs, slab couldn't reach at the bottom of the solution box. Consequently, the surface respond and amount of trench retreat remain low comparing the other tests.

RET-11 experiment is critical because the slab has nearly reached at the bottom of the solution box at t = 25.5 Myrs. At RET-9, there was a retreat amount anomaly at t = 18.5 Myrs, corresponds to the time when slab reached to the bottom of the box, triggered an increase at the retreat amount and also at the crustal and lithospheric thinning. Ablation time and amount also increses with slab density. While there was almost none ablation can be seen at RET-9 by t = 25.5 Myrs, the ablation at RET-11 was started by t = 18.5 Myrs and the amount of ablative material has reached nearly 260 km deep below the surface.

As a result, the highest amount of retreat and β factor for back-arc was calculated at densest ocean slab model (RET-15). It can be seen that oceanic slab density can directly be correlated with the amount of trench retreat and β factor at the continental crust. While the density difference between subducting slab and asthenosphere

increases, the oceanic material tend to sink into the asthenosphere and greatly increases the slab pull force (F_{sp}), as well as amount of extension.

Table 3.3 Model results of Subducting lithosphere density

| Model	Retreat	Max. Sub	Cru. Thick	Lith. Thick	β factor
RET-9	370 km	3.1 km	29 km	65 km	1.37
RET-10	373 km	3.3 km	27 km	62 km	1.48
RET-11	375 km	3.35 km	26 km	60 km	1.53
RET-12	377 km	3.9 km	25 km	57 km	1.6
RET-13	380 km	4.2 km	24.5 km	55 km	1.63
RET-14	390 km	4.3 km	24 km	54 km	1.66
RET-15	410 km	5.1 km	23 km	52 km	1.74
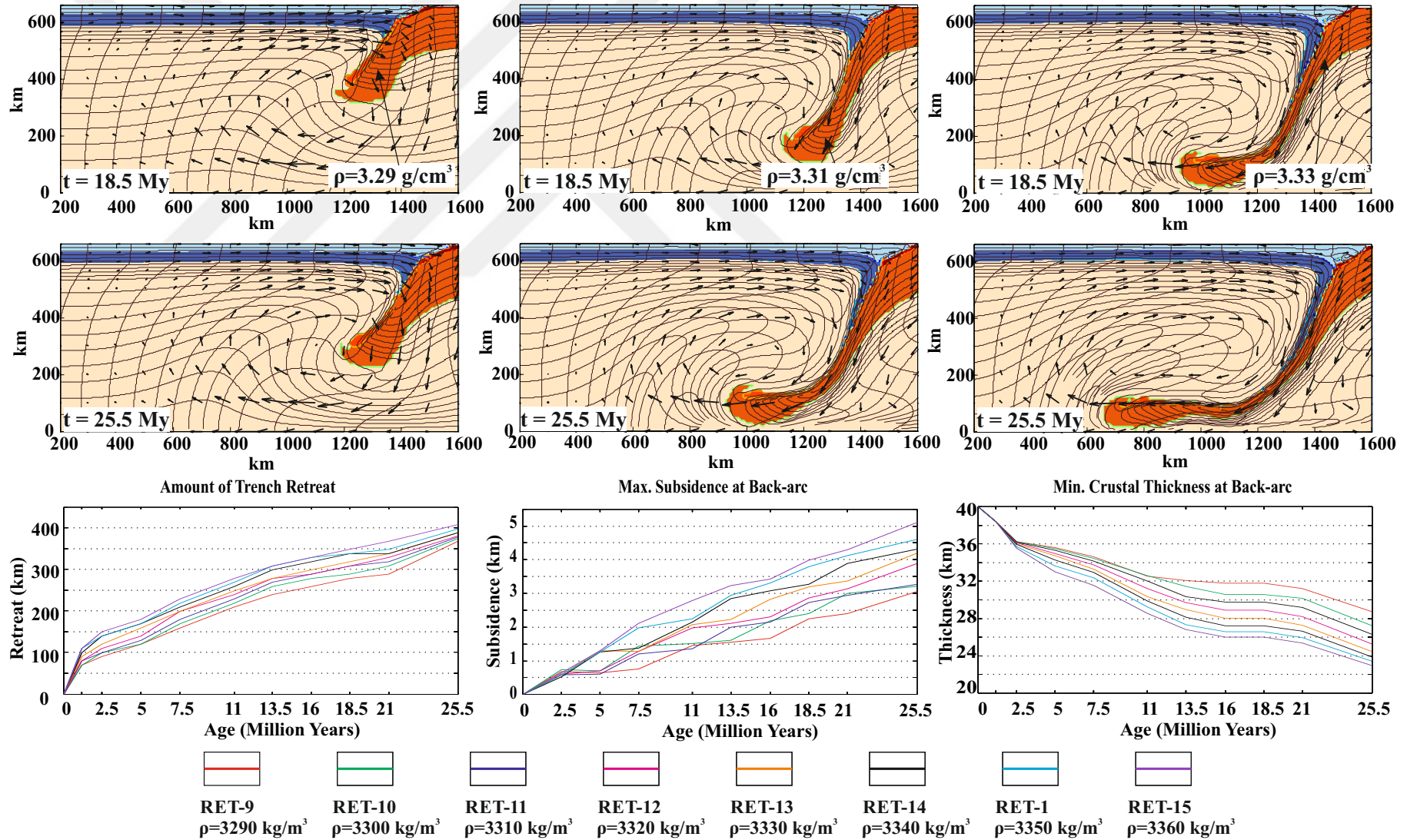
Figure 3.4 : Models with different oceanic lithosphere densities Increasing slab density increases the amount of retreat and the deformation of the back-arc lithosphere.

3.4   The Effect of Convergence Velocity

It is predicted that the average subduction velocity is 1 cm/year at Hellenic trench due to predictions of Jolivet & Faccenna (2000) but the convergence velocity in models was changed in order to understand its effect on trench retreat. Starting model has 1 cm/year velocity, models with 0 cm/year (RET-16), 0.25 cm/year (RET-17), 0.5 cm/year (RET-18), 0.75 cm/year (RET-19), 1.25 cm/year (RET-20) and 1.5 cm/year (RET-21) were tested.

By looking the test results, it can be seen that the effect of convergence velocity is the minor component of the retreating trench system. All of the models start with the same trend and reach 100-120 km in 1.25 Myrs. While the highest amount of retreat was calculated at RET-16, lowest amount at RET-21. This means increasing convergence velocity decreases the amount of retreat and the maximum subsidence. At the same time with the decreasing convergence velocity, deformation of the back-arc crust and lithospheric mantle is slightly increases. Crustal thining values differ between 23-24 km.

Model	Retreat	Max. Sub	Cru. Thick	Lith. Thick	β factor
RET-16	440 km	3.7 km	23 km	53 km	1.74
RET-17	430 km	3.6 km	23.2 km	53.2 km	1.72
RET-18	425 km	3.5 km	23.4 km	53.4 km	1.71
RET-19	410 km	3.45 km	23.6 km	53.6 km	1.69
RET-20	375 km	3.35 km	23.8 km	53.8 km	1.68
RET-21	370 km	3.3 km	24 km	54 km	1.66
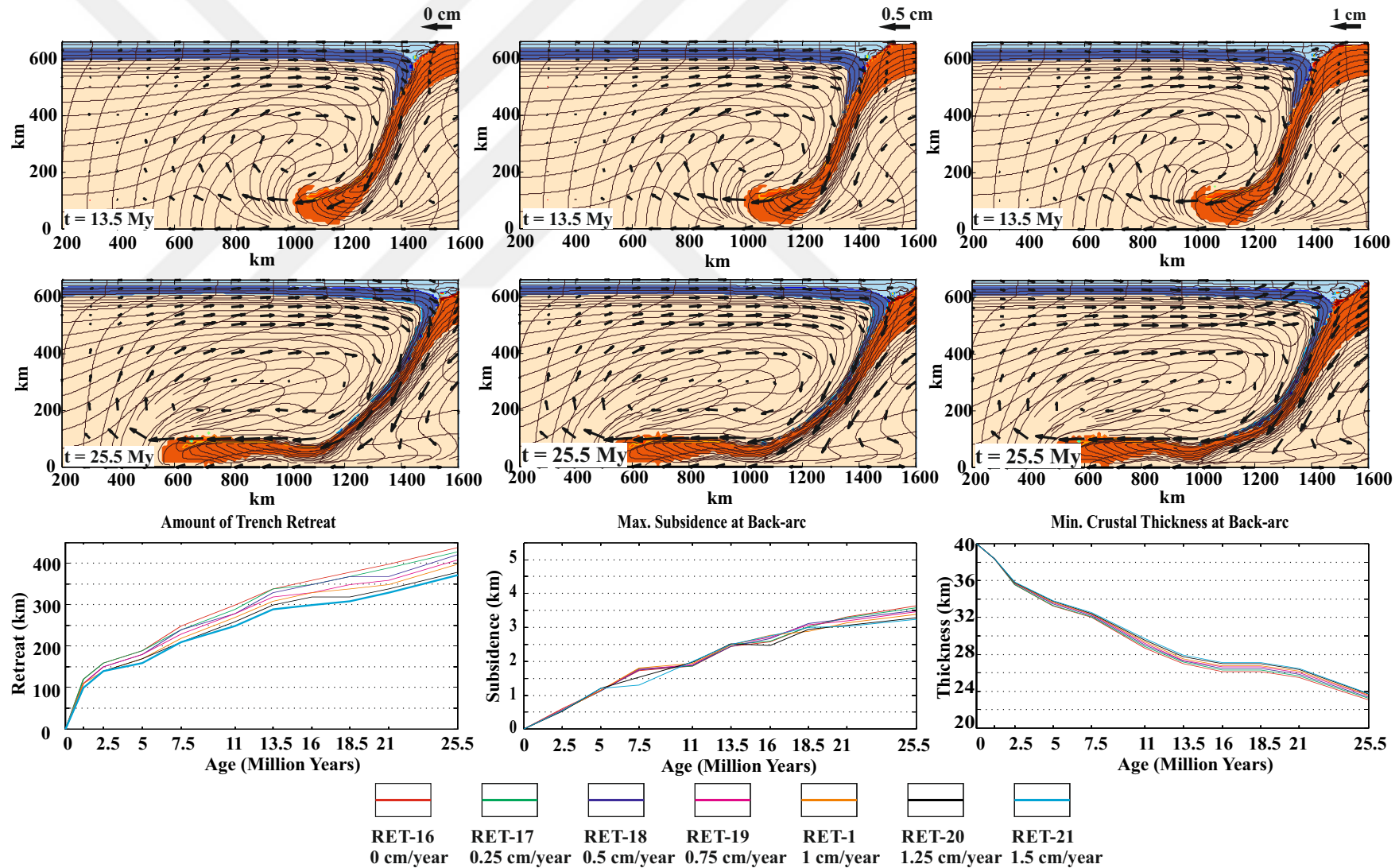
Figure 3.5 : Effect of convergence velocity. Increasing convergence velocity decreases the amount of trench retreat and the deformation at the back-arc lithopshere

3.5   Uniform Lithosphere Thickness Tests

In previous tests, it is noted that lithosphere thicknesses are important for back-arc extension, both continental and oceanic. In order to understand which lithosphere is more effective on back-arc extension; some other experiments were conducted using uniform lithosphere thicknesses, same thickness for both continental and oceanic lithosphere. It is rational to correlate uniform 80 km thickness (RET-22) with uniform 120 km (RET-26), likewise 90 km thickness (RET-23) with 110 km thickness (RET-25) because these two sets are equidistant from RET-24 (100 km uniform lithospheric thickness).

First, RET-24 (100 km continental, 100 km ocean lithosphere thickness) was conducted and correalated with RET-1. RET-22 has thinner back-arc lithosphere thickness and was indicated higher streching rates as expected. But if RET-22 is correlated with RET-26, it can be seen that streching increases at back-arc while both lithosphere thicknesses (continent – ocean) are increasing. Thicker continental lithosphere couldn't resist the slab pull force imposed by a thick ocean lithosphere. Likewise, the correlation of RET-23 and RET-25 gives similar result. The maximum amount of deformation is calculated at RET-26 model. It has 450 km trench retreat and 3.6 km max. subsidence. According to these results, role of retreating oceanic lithosphere thickness is more significant than back-arc lithosphere thickness. It is worthwhile to note that; RET-22, RET-23 and RET-24 gives similar results comparing to other two models. There seems be two similar paterns at amount of retreat graph. That means 100 km lithosphere thickness is critical for retreating trench geodynamics.
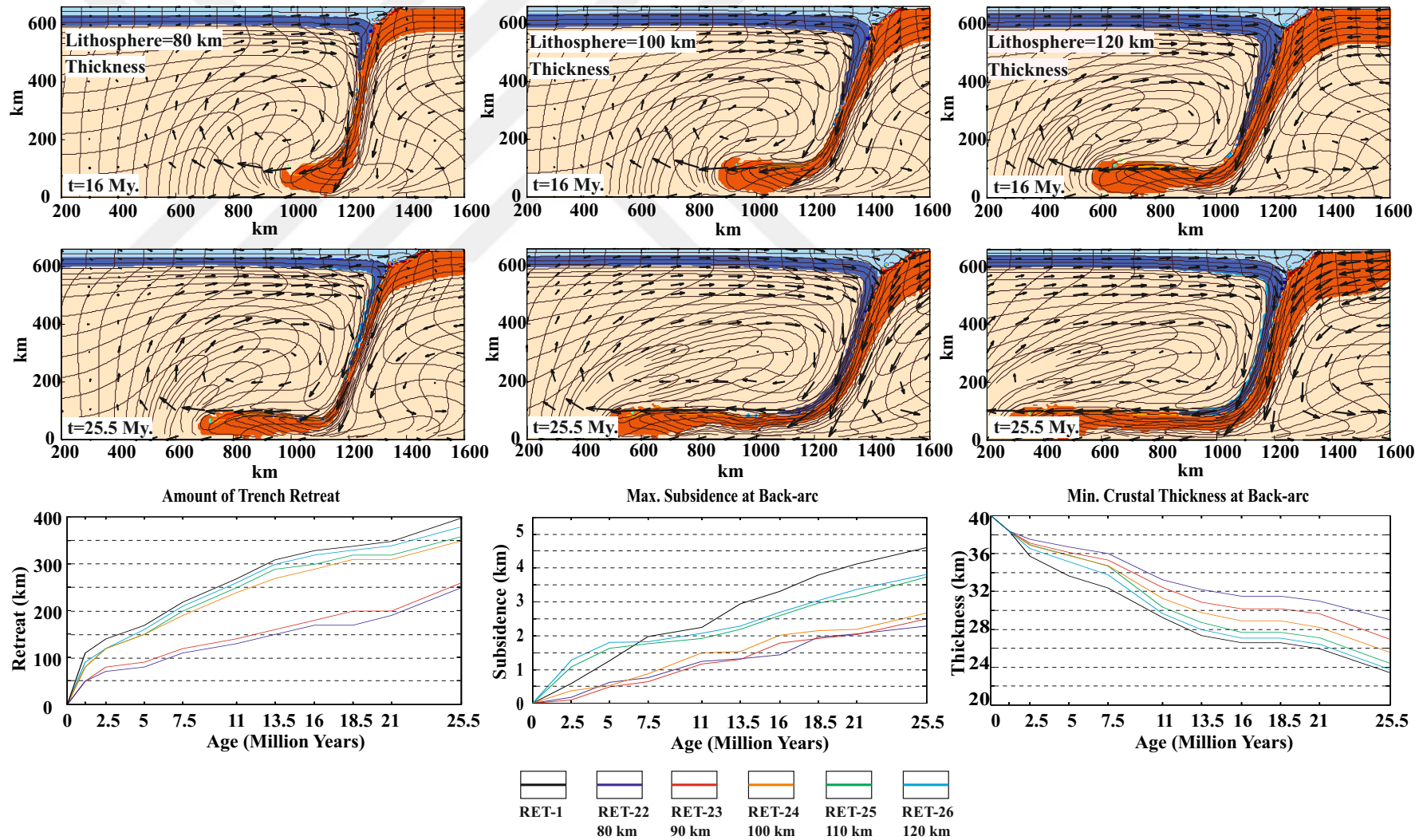
Figure 3.6 : Models with uniform lithosphere thicknesses. Continental and oceanic lithosphere thicknesses are selected equal.

3.6   The Effect of Moho Temperature

Moho depth is defined as unconformity between crust and mantle lithosphere. This imaginary surface has its own temperature at different areas, for example in active volcanic regions, Moho temperature may be higher but inside cratons like Siberia or Canada, temperatures tend to be low because of thick crust and lithosphere. Sonder et al (1987) indicated that lithsophere may behave different in various temperature profiles. Starting from this point of view, models with different Moho temperatures were constructed to see its effect for back-arc deformation. Starting model (RET-1) has 650^0C moho temperature and models with 500^0C (RET-27), 550^0C (RET-28), 600^0C (RET-29), 700^0C (RET-30), 750^0C (RET-31), 800^0C (RET-32), 850^0C (RET-33), 900^0C (RET-34) and 950^0C (RET-35) were conducted.

These model results indicate that different moho temperatures in thin continental lithosphere has almost no effect to the extension or the deformation at the back-arc. The only difference is the slab geometry. At colder moho temperatures, sinking slab tends to bend downwards with the gravitational force (Figure 3.7).
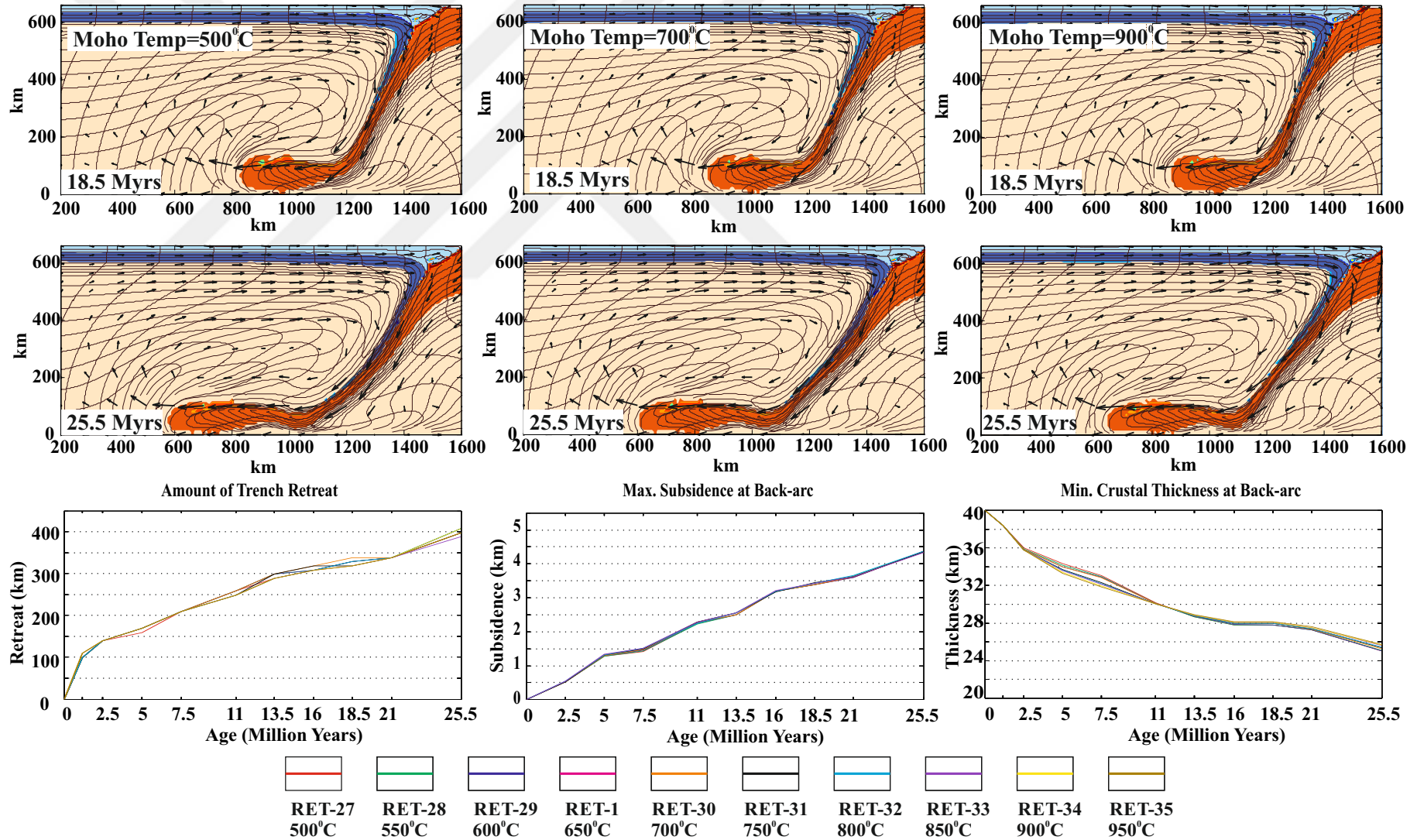
Figure 3.7 : Models with different back-arc moho temperatures. There is no important change occurs with different moho temperatures.

Similar set of experiments were conducted with thicker back-arc lihosphere (150 km total). With thicker lithosphere, effect of the moho temperature can be seen more easily.

It is important to note that the results are close for each moho temperature model. Retreat and back-arc crustal thinning amounts seems like consistent. It is clear that the amount of trench retreat is slowly decreased with increasing back-arc temperature profile. The problem with this set of models, maximum subsidence values at back arc are not well matched with retreat and crustal thinning amounts. According to Airy isostacy, high topography should have supported by thick crust and lithosphere. This problem may be a result of changing behavior of continental lithosphere due to changing Moho temperature. If Moho temperature is high, that means heat flux through mantle lithosphere will be lower. At some values, lithosphere may easily deforms otherwise don't. Higher than 650^0C moho temperature, the slab is getting deformed and imbricated at 660 km depth (Figure 3.8). Also the material coming from continental lithosphere is decreased. That means ablative subduction may have interrupted. Lithosphere resists deformation at shallow levels, which makes the slab steeper ($\sim 80^0$).

This means there must be a thick lithosphere to measure the effect of moho temperature. While the thicker lithosphere gets deformed under different moho temperatures, thinner lithosphere mostly deformed under the effect of slab pull force. The deformation applied by the dense subducting lithosphere is so dominant, the difference created by moho temperature can be negligent.
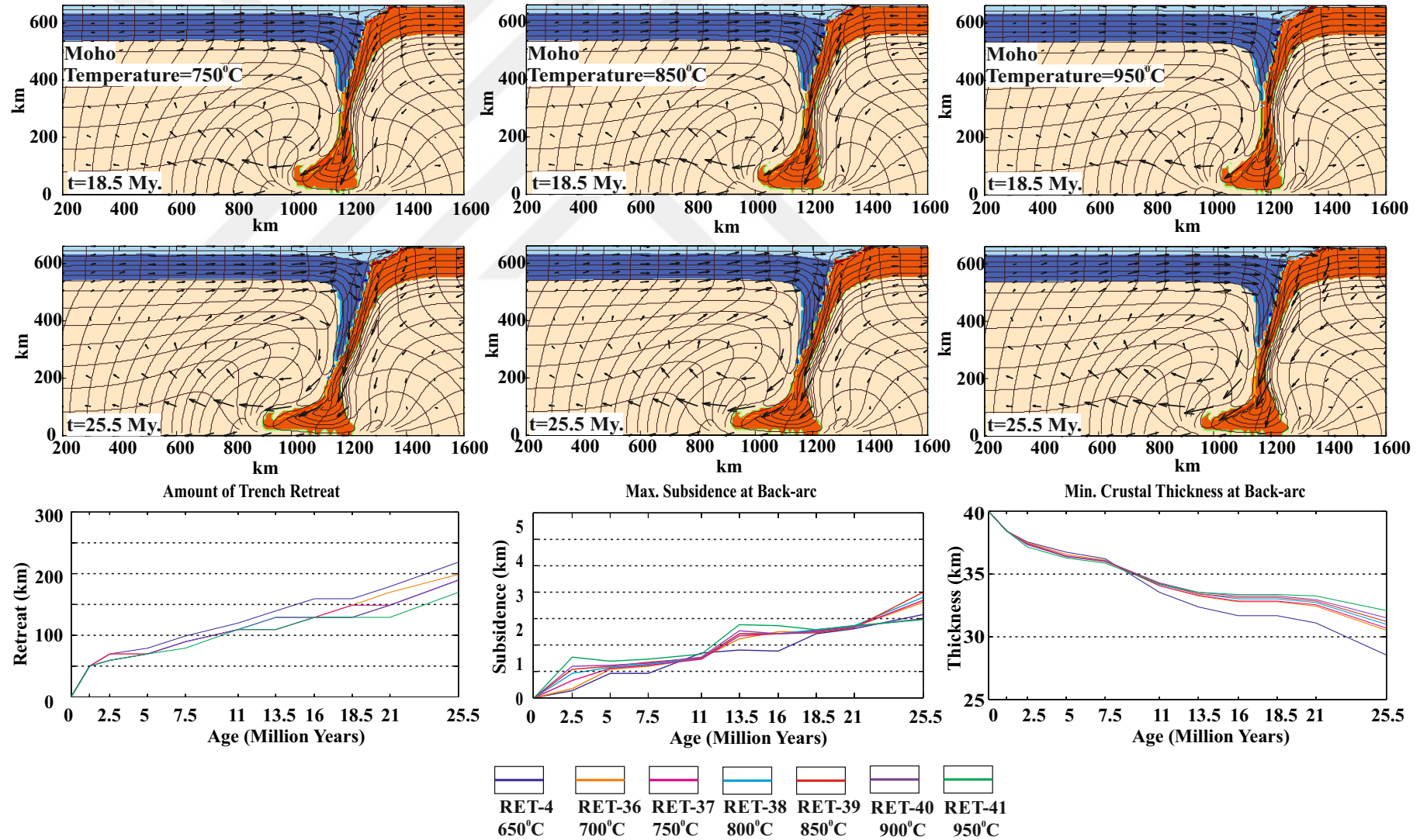
Figure 3.8 : Moho Temperature test results with thicker lithosphere (150 km total thickness). Distinctly from other moho temperature tests, different temperatures changes the amount of retreat and deformation at the back-arc.

3.7   Slab Break-off Models

While mantle tomography studies show continous subducting slab beneath Aegean region, the slab beneath Western Anatolia (Van Hinsbergen et al., 2010). This discontinuity is interpreted as a slab tear or slab window. At these images, the teared part of the ocean lithosphere was appeared under SW Anatolia. And also the age of volcanism (Late Miocene, ~5-10 Myrs) is interpreted as breakage age. In this set of experiments the slab break-off models were conducted in order to understand its effect to the back-arc. To construct this experiment, a very dense and deformed oceanic lithosphere was used for the edge of the slab and no velocity was imposed. Models were conducted for 7.5 Myrs. These models were correlated with their none break-off conjugates. BOFF-1 model will be correlated with RET-23 (90 km ocean – continent), BOFF-2 (100 km ocean – continent) with RET-24 and BOFF-3 with RET-4 (100 km ocean, 150 km continent).

At BOFF-1; 90 km oceanic, 90 km continental material were used. After 1.25 Myrs, break-off has occurred and the slab was started to sink into the asthenosphere. With the slab detachment, the material field of the model come up like a collision. The remaining piece has bended into asthenosphere because of its density. Also by t = 3.75 Myrs, the sinking ocean lithosphere started due to small scale convection within the asthenosphere. These movements cause some deformation at back arc. At t = 7.5 Myrs, the detached piece was reached to bottom of the solution box. The other two break-off models give similar results, depend on their lithospheric properties. For example if BOFF-2 and RET-16 were correlated, each of these models come up with similar trench migration amounts. The other set; BOFF-3 and RET-17 reveals corresponding results. The overall difference between two sets are caused by lithsopheric thickness variations. In conclusion, break-off event cannot cause much effect to the back-arc lithosphere (Figure 3.10).
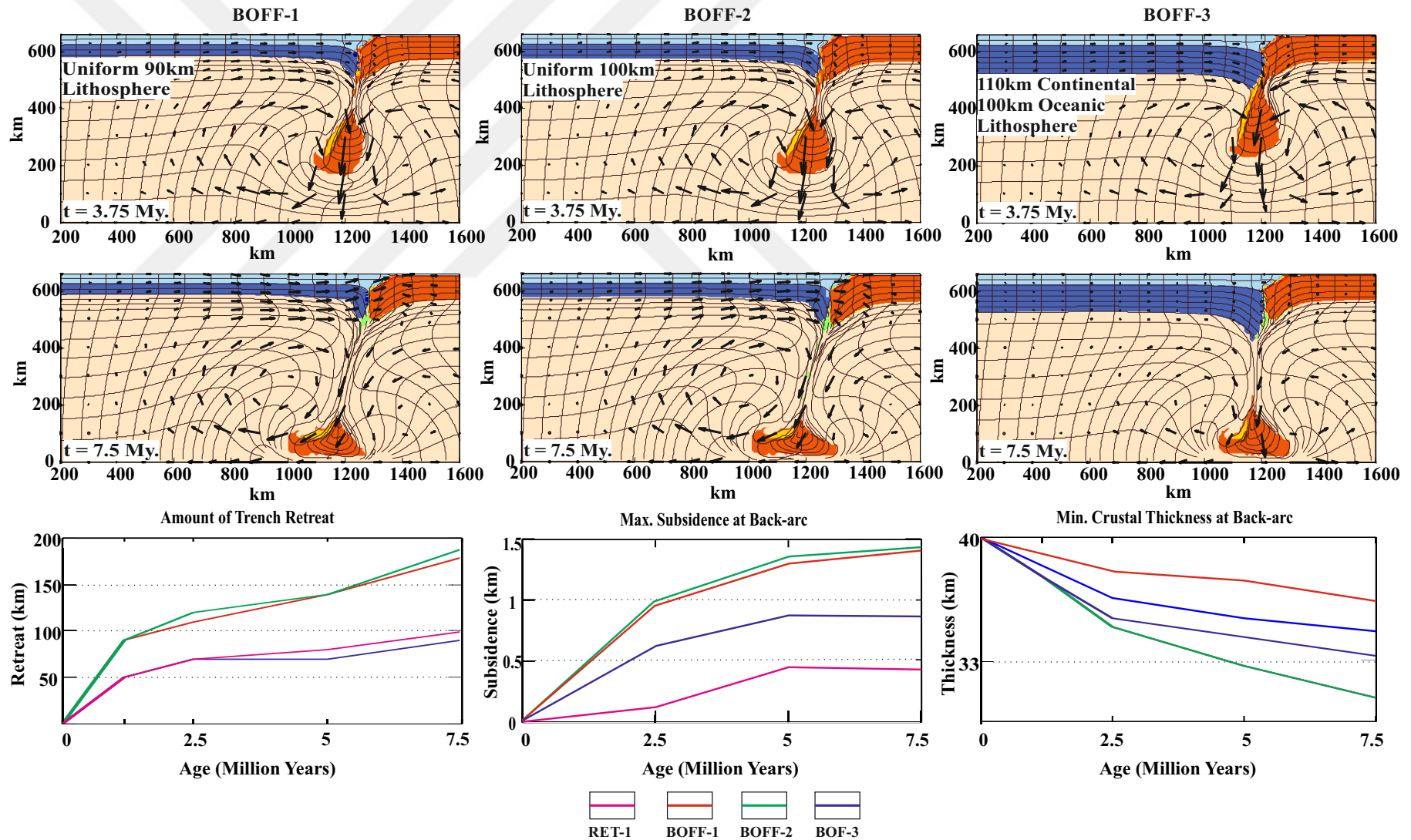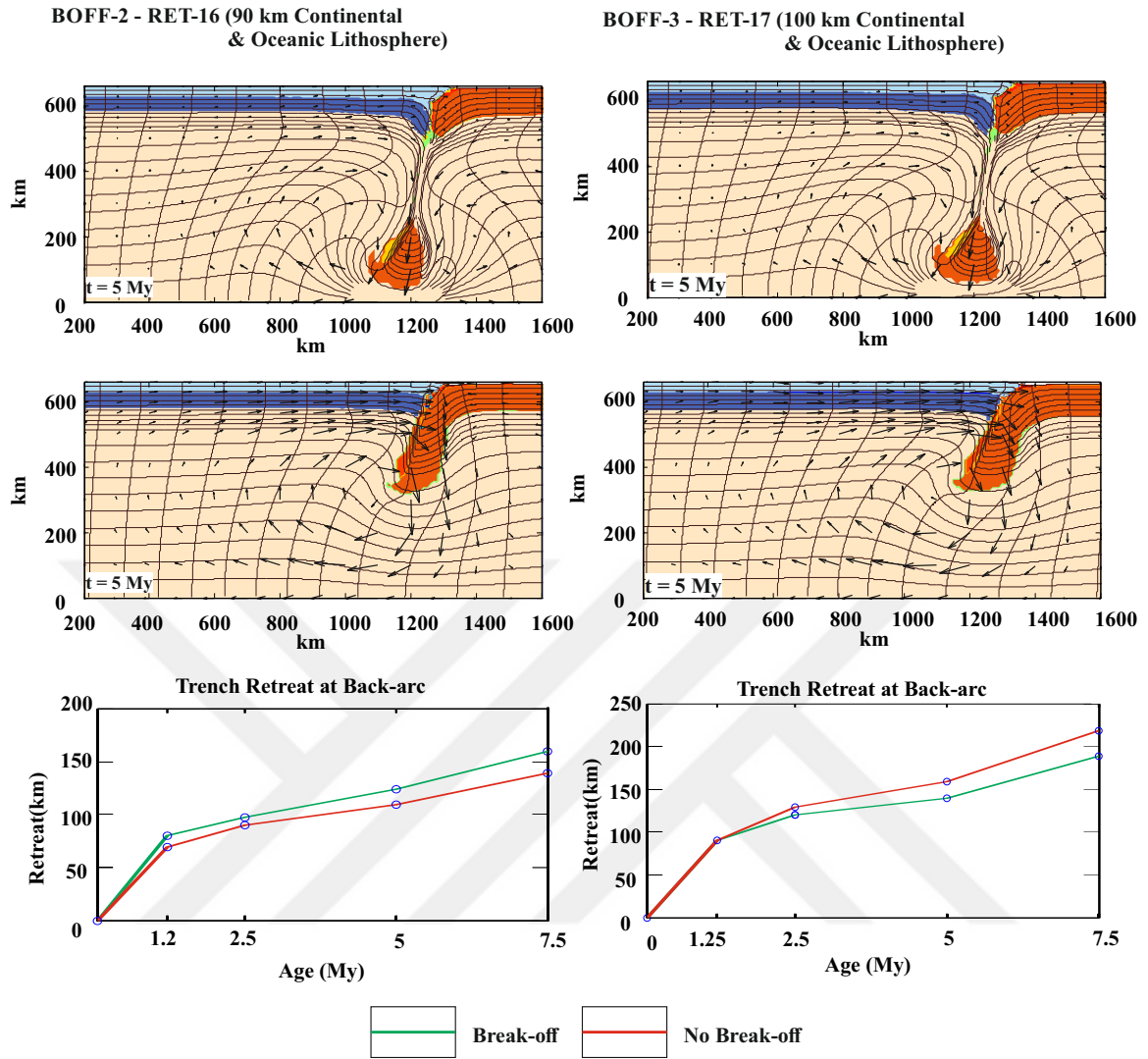
Figure 3.9 : Slab break-off models for 7.5 My. There is no distinct difference between the break-off and non break-off.

Figure 3.10 : Slab Break-off model comparisons with their none break-off conjugates.

4 DISCUSSION AND CONCLUSION

4.1 Retreat Amount Comparison

According to former studies, the Aegean trench was migrated 400 km to SW-SSW (Faccenna et al., 2014). Models conducted here reveal maximum 400 km retreat in 50 km mantle lithosphere thickness experiment (RET-1) and 430 km retreat in 120 km oceanic lithosphere thickness test (RET-8) (Figure 4.2). It is also noted that lithosphere thicknesses are the main driving parameter for the retreat mechanism. Both continental and oceanic lithosphere are playing significant role on deformation caused by trench retreat. For example, the model with thicker back-arc lithosphere (RET-3) generates 280 km trench retreat, model with thinner back-arc lithosphere (RET-2) up to 320 km.

4.2 Maximum Subsidence Comparison

It has been calculated that the maximum subsidence at back-arc around $1.5 - 4.5$ km. By looking the seismic data, the thickness of the sediment load was found in the range of $2.5 - 3$ km in Gediz Graben (Yılmaz et al., 2000) and more then 2 km in the Menderes Massif (Sari & Şalk, 2004). In Aegean Sea, the amount of sediment is around 3.5 km (Makris, 1975). While thin back-arc lithosphere thickness models may explain the Aegean Sea extension, models with thick continental mantle lithosphere corresponds more likely to Western Anatolia. 150 km thick lithoshere model (RET-4) shows 2.3 km maximum subsidence at back-arc (Figure 4.3).

4.3 Crustal and Lithospheric Thickness Comparison

90 km thick lithosphere thickness model (RET-1) results show around 22.75 km thick crust, β factor around 1.75 and 110 km lithosphere thickness model results indicate around 25.75 km thick crustal ($\beta=1.55$). Geophysical measurements indicate that average crustal thickness in the Aegean region is 25 km (Sodoudi et al., 2006) and the predictions of Le Pichon & Angelier (1981) demonstrate β factor is up to

1.58 for Aegean Sea. Besides that lithosphere thickness was calculated around 90-100 km at Western Anatolia region N-S cross section (Kind et al., 2015) and models were indicate around 90-110 km (RET-3, 4). If there was relatively thin lithosphere (~90 km) in the Aegean Sea about 25 million years ago or somehow thinned down via convective removal, a continuous slab retreat may produce this extension. Thin continental lithosphere can easily be deformed and supports trench retreat.
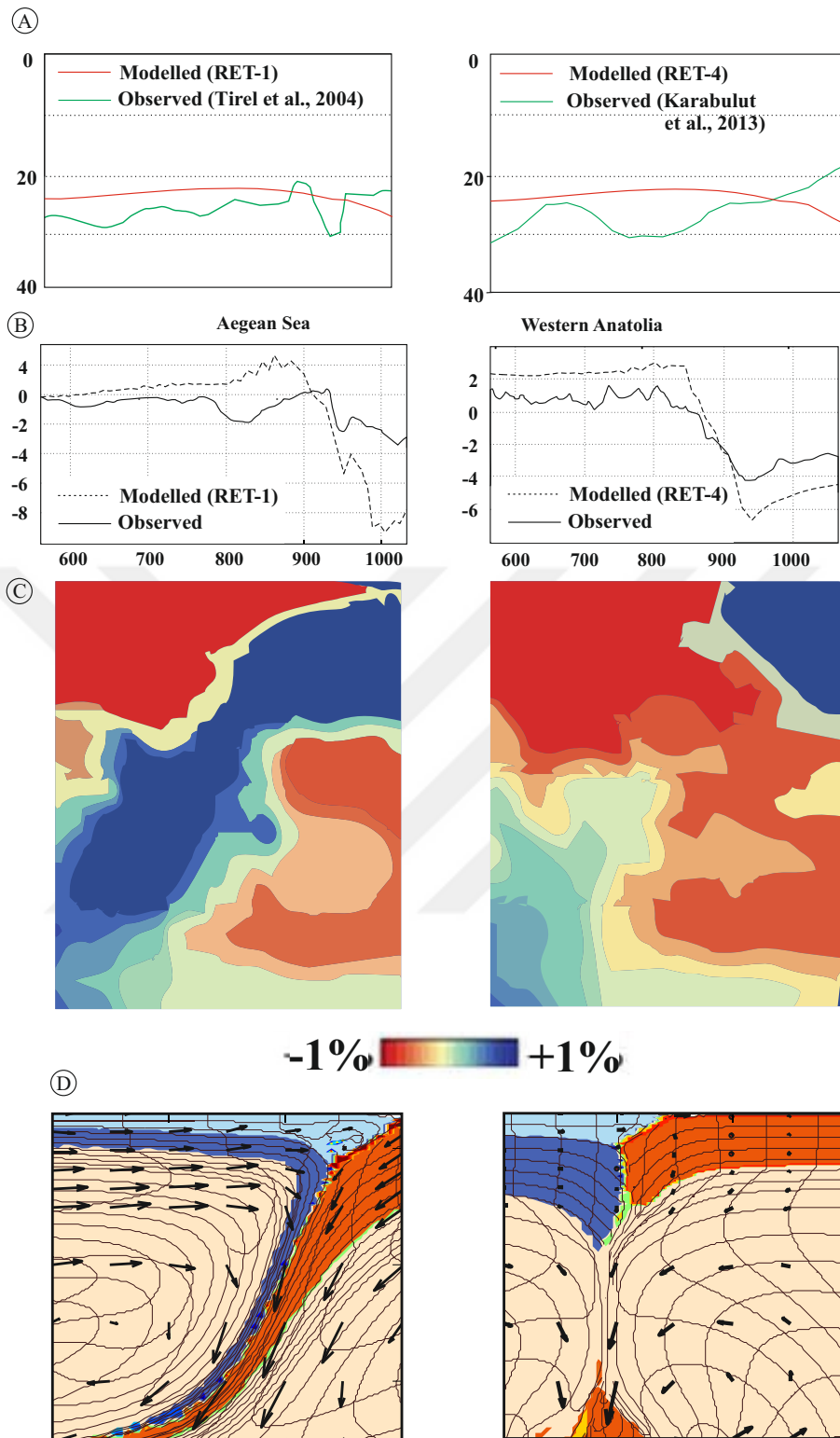
Figure 4.1 : A) Crustal thickness comparisons of Aegean Sea (Left) (From Tirel et al., 2004) and Western Anatolia (Right) (Karabulut et al., 2013). B)Topography profiles. C) Seismic tomography images (Van Hinsbergen., 2010). D) Material fields of RET-1 and RET-4
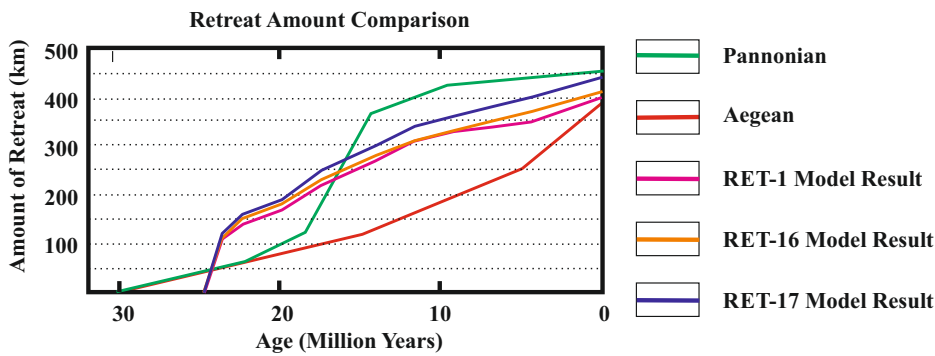
Figure 4.2 : Amount of retreat comparison.
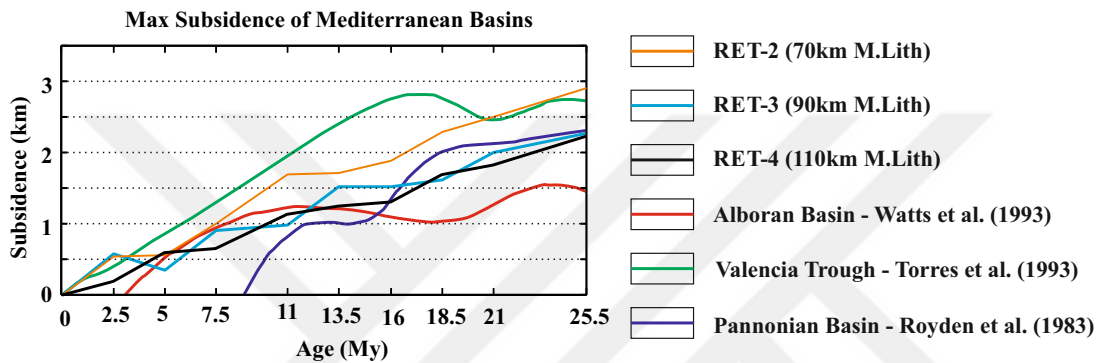
Figure 4.3 : Amount of subsidence comparison.

4.4 Proposed Model for Aegean Sea and Western Anatolia

The models show that slab break-off is not significant in terms of extension. If Paleocene compression might have affected the lithosphere of Western Anatolia more than the lithosphere of Aegean Sea, there should have developed a thickness difference between these two. Continental lithsophere thickness models indicate that thicker overriding plate is less likely to extend, so the slab beneath Western Anatolia could not retreat easily with respect to slab beneath Aegean Sea. So there should be a shear zone within the ocean slab. The slab tear was developed within this counterclockwise shear zone, triggered the inflow of asthenosphere, started from the slab margin, moved towards the center (Figure 4.3). The first alkaline Neogene volcanism at Isparta triangle was triggered by tear. Its surficial response may corresponds to SW – NE shear zone at east of Rhodes (Özbakır et al., 2013). The stress vector increases at the plate margin within the teared area. That's why the size of the lithospheric gap increases with time towards the center of the slab. The gravitational force of the whole subducting lithosphere is concentrated in still continous part of the slab which also triggers tear and trench migration. According to

this interpretation, slab tear is not a cause, its an effect. Volcanism data also show that Isparta volcanics (where the tear is predicted) has age of 6-4 Ma (Ersoy & Palmer, 2013) and this corresponds to tear event. At break-off models show the remnant of the slab still sinking beneath asthenosphere just like the tomography images (Van Hinsbergen et al., 2010) (Figure 4.4).

At oceanic lithosphere thickness tests, more back-arc deformation is determined if the oceanic lithosphere is thick. So the subducting slab has more enforcement than other parameters. The slab pull force is vastly increased because of its weight. Oceanic lithosphere thickness is the triggering parameter for the slab rollback.

As a result, the amounts of maximum subsidence, retreat and β factor for back-arc are consistent with Mediterranean basins. Trench migration may generate enough deformation. Retreating Hellenic trench may explain the extensional tectonics that we see today at Aegean Sea.
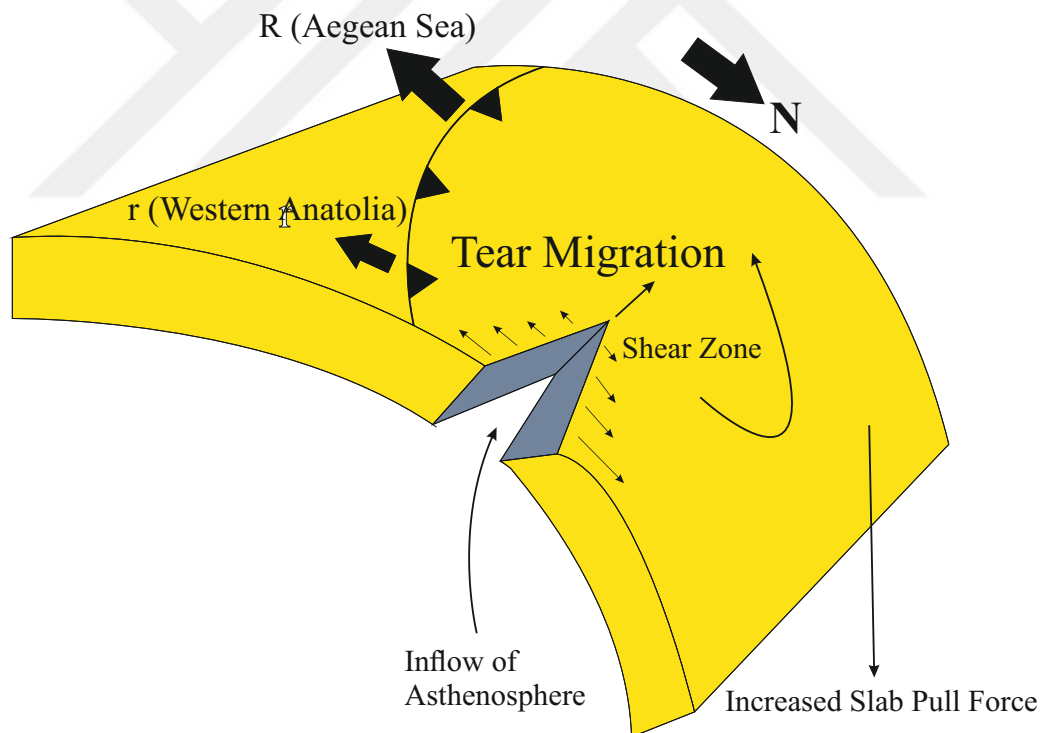
Figure 4.4 : Proposed model for Aegean Sea and Western Anatolia. "R" is the vector shows faster rate of retreat. The different amounts of retreat cause shear within the oceanic plate and deforms it. The tear is produced along this deformation zone through the center of the slab.
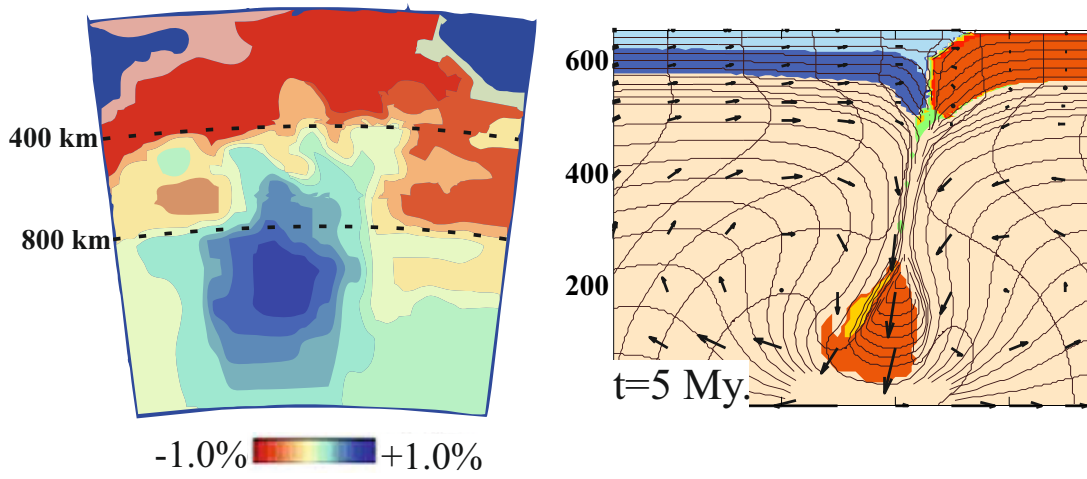
Sinking Time Comparison

Figure 4.5 : Sinking time comparison.

5   REFERENCES

Aktug, B., Nocquet, J. M., Cingöz, A., Parsons, B., Erkan, Y., England, P., ... & Tekgül, A. (2009). Deformation of western Turkey from a combination of permanent and campaign GPS data: Limits to block-like behavior. *Journal of Geophysical Research: Solid Earth, 114*(B10).

Aldanmaz, E., Pearce, J.A., Thirlwall, M.F., Mitchell, J.G., (2000). Petrogenetic evolution of late Cenozoic , post-collision volcanism in western Anatolia , Turkey. J. Volcanol. Geotherm. Res. 102, 67–95.

Biryol, B.C., Beck, S.L., Zandt, G., Özacar, A.A., (2011). Segmented African lithosphere beneath the Anatolian region inferred from teleseismic P-wave tomography. Geophys. J. Int. 184, 1037–1057. doi:10.1111/j.1365-246X.2010.04910.x

Bozkurt, E., Sözbilir, H., (2004). Tectonic evolution of the Gediz Graben: field evidence for an episodic, two-stage extension in western Turkey. Geol. Mag. 141, 63–79. doi:10.1017/S0016756803008379

Çoban, H., Karacık, Z., Ece, Ö.I., (2012). Source contamination and tectonomagmatic signals of overlapping Early to Middle Miocene orogenic magmas associated with shallow continental subduction and asthenospheric mantle flows in Western Anatolia: A record from Simav (Kütahya) region. Lithos 140-141, 119–141. doi:10.1016/j.lithos.2011.12.006

Dilek, Y., Altunkaynak, Ş., (2009). Geochemical and temporal evolution of Cenozoic magmatism in western Turkey : mantle response to collision , slab break-off , and lithospheric tearing in an orogenic belt. Geol. Soc. London 311, 213–233. doi:10.1144/SP311.8

Dewey, J.F., Şengör, A.M.C., (1979). Aegean and surrounding regions: Complex multiplate and continuum tectonics in a convergent zone. Geol. Soc. Am. Bull. 90, 84–92. doi:10.1130/0016-7606(1979)90<84:AASRCM>2.0.CO;2

Edwards, M.A., Grasemann, B., (2009). Geological Society , London , Special Publications Mediterranean snapshots of accelerated slab retreat : subduction instability in stalled continental collision service Mediterranean snapshots of accelerated slab retreat : subduction instability in stalle. Geol. Soc. London 311, 155–192. doi:10.1144/SP311.6

Eleftheriadis, G., Christofides, G., Kassoli-Fournaraki, A. (1984). Geochemistry of the high-K calc-alkaline basaltic sills and dykes in the South Rhodope Massif (N Greece). *Bulletin Volcanologique, 47*(3), 569-579.

Emre, T., & Sözbilir, H., (1997). Field evidence for metamorphic core complex, detachment faulting and accommodation faults in the Gediz and Büyük Menderes grabens, western Anatolia. In *International Earth Sciences Colloquium on the Aegean Region, Izmir-Güllük, Turkey*. 73-93.

Emre, T., & Sözbilir, H. (2005). Geology, Geochemistry and Geochronology of the Başova Andesite, Eastern end of the Küçük Menderes Graben. *Mineral Research and Exploration of Turkey (MTA) Bulletin*, *131*, 1-19.

Ercan, T., Satir, M., Kreuzer, H., Türkecan, A., Günay, E., Çevikbaş, A., Ateş, M., Can, B., (1985). Batı Anadolu Senozoyik volkanitlerine ait yeni kimyasal , izotopik ve radyometrik verilerin yorumu. Türkiye Jeol. Kongresi 28, 121–136.

Ercan, T., Satir, M., Steinitz, G., Dora, A., Sarıfakıoğlu, E., Adls, C., Walter, H.-J., Yıldırım, T., (1995). Biga yarımadası ile Gökçeada , Bozcaada ve Tavşan adalarındaki (KB Anadolu) Tersiyer Volkanizmasının Özellikleri. MTA 117, 55–86.

Ersoy, E. Y., & Palmer, M. R. (2013). Eocene-Quaternary magmatic activity in the Aegean: implications for mantle metasomatism and magma genesis in an evolving orogeny. *Lithos*, *180*, 5-24.

Faccenna, C., Becker, T. W., Auer, L., Billi, A., Boschi, L., Brun, J. P., ... & Piromallo, C. (2014). Mantle dynamics in the Mediterranean. *Reviews of Geophysics*, *52*(3), 283-332.

Fullsack, P., (1995). An arbitrary Lagrangian-Eulerian formulation for creeping flows and its application in tectonic models. Geophys. J. Int. 120, 1–23. doi:10.1111/j.1365-246X.1995.tb05908.x

Fytikas, M., Giuliani, O., Innocenti, F., Manetti, P., Mazzuoli, R., Peccerillo, A., & Villari, L. (1979). Neogene volcanism of the northern and central Aegean region. *Ann. Géol. Pays Hell*, *30*(1), 106-129.

Fytikas, M., Innocenti, F., Manetti, P., Peccerillo, A., Mazzuoli, R., Villari, L., (1984). Tertiary to Quaternary evolution of volcanism in the Aegean region. Geol. Soc. London, Spec. Publ. doi:10.1144/GSL.SP.1984.017.01.55

Hatzipanagiotou, K., & Pe-Piper, G. (1995). Ophiolitic and sub-ophiolitic metamorphic rocks of the Vatera area, southern Lesbos (Greece): geochemistry and geochronology. *Ofioliti*, *20*(1), 17-29.

Heuret, A., & Lallemand, S. (2005). Plate motions, slab dynamics and back-arc deformation. *Physics of the Earth and Planetary Interiors*, *149*(1), 31-51.

Innocenti, F., Agostini, S., Vincenzo, G. Di, (2005). Neogene and Quaternary volcanism in Western Anatolia: magma sources and geodynamic evolution. Mar. Geol. 221, 397–421. doi:10.1016/j.margeo.2005.03.016

Jarrard, R. D. (1986). Relations among subduction parameters. *Reviews of Geophysics*, *24*(2), 217-284.

Jolivet, L., Faccenna, C., (2000). Mediterranean extension and the Africa-Eurasia collision. Tectonics 19, 1095–1106.

Jolivet, L., Faccenna, C., Huet, B., Labrousse, L., Le Pourhiet, L., Lacombe, O., ... & Philippon, M. (2013). Aegean tectonics: Strain localisation, slab tearing and trench retreat. *Tectonophysics*, *597*, 1-33.

Karabulut, H., Paul, A., Ergün, T.A., Hatzfeld, D., Childs, D.M., Aktar, M., (2013). Long-wavelength undulations of the seismic Moho beneath the strongly stretched Western Anatolia. Geophys. J. Int. 194, 450–464. doi:10.1093/gji/ggt100

Karaoğlu, Ö., Helvaci, C., Ersoy, Y., (2010). Petrogenesis and 40Ar/39Ar geochronology of the volcanic rocks of the Uşak-Güre basin, western Türkiye. Lithos 119, 193–210. doi:10.1016/j.lithos.2010.07.001

Kind, R., Eken, T., Tilmann, F., Sodoudi, F., Taymaz, T., Bulut, F., (2015). Thickness of the lithosphere beneath Anatolia from S receiver functions. Solid Earth 17, 3527. doi:10.5194/sed-7-1315-2015

Krushensky, R. D. (1976). Volcanic rocks of Turkey. *Bulletin of Geological Survey, Japan*, *26*, 393-412.

Le Pichon, X., Angelier, J., Osmaston, M.F., Stegena, L., 1981. The Aegean Sea. Philos. Trans. R. Soc. London. A Math. Phys. Sci. 300, 357–372. doi:10.1098/rsta.1981.0069

Makris, J. (1975). Crustal structure of the Aegean Sea and the Hellenides obtained from geophysical surveys. *J. Geophys*, *41*, 441-443.

Marchev, P., Kaiser-Rohrmeier, M., Heinrich, C., Ovtcharova, M., von Quadt, A., Raicheva, R., (2005). 2: Hydrothermal ore deposits related to post-orogenic extensional magmatism and core complex formation: The Rhodope Massif of Bulgaria and Greece. Ore Geol. Rev. 27, 53–89. doi:10.1016/j.oregeorev.2005.07.027

McKenzie, D., Weiss, N., (1975). Speculations on the Thermal and Tectonic History of the Earth. Geophys. J. R. Astron. Soc. 42, 131–174. doi:10.1111/j.1365-246X.1975.tb05855.x

Meulenkamp, J.E., Wortel, M.J.R., van Wamel, W. a., Spakman, W., Hoogerduyn Strating, E., (1988). On the Hellenic subduction zone and the geodynamic evolution of Crete since the late Middle Miocene. Tectonophysics 146, 203–215. doi:10.1016/0040-1951(88)90091-1

Mutlu, A.K., Karabulut, H., (2011). Anisotropic Pn tomography of Turkey and adjacent regions. Geophys. J. Int. 187, 1743–1758. doi:10.1111/j.1365-246X.2011.05235.x

Okay, A. I., Siyako, M., & Bürkan, K. A. (1991). Geology and tectonic evolution of the Biga Peninsula, northwest Turkey. *Bulletin of the Technical University of Istanbul*, *44*(1-2), 191-256.

Okay, A. I., Harris, N. B., & Kelley, S. P. (1998). Exhumation of blueschists along a Tethyan suture in northwest Turkey. *Tectonophysics*, *285*(3), 275-299.

Okay, A.I., Satir, M., (2000). Coeval plutonism and metamorphism in a latest Oligocene metamorphic core complex in northwest Turkey. Geol. Mag. 137, 495–516. doi:10.1017/S0016756800004532

Okay, A. I. (2001). Stratigraphic and metamorphic inversions in the central Menderes Massif: a new structural model. *International Journal of Earth Sciences*, *89*(4), 709-727.

Özbakır, A. D., Şengör, A. M. C., Wortel, M. J. R., & Govers, R. (2013). The Pliny–Strabo trench region: A large shear zone resulting from slab tearing. *Earth and Planetary Science Letters*, *375*, 188-195.

Pasyanos, M. E. (2010). Lithospheric thickness modeled from long-period surface wave dispersion. *Tectonophysics*, *481*(1), 38-50.

Paul, A., Salaün, G., Karabulut, H., Pedersen, H. A., & Kömec Mutlu, A. (2012, April). Traces of subduction and their relation to seismic anisotropy beneath Greece and Turkey: New evidences and questions from seismic tomography. In *EGU General Assembly Conference Abstracts* (Vol. 14, p. 2913).

Peltier, W. R. (1986). Deglaciation-induced vertical motion of the North American continent and transient lower mantle rheology. *Journal of Geophysical Research: Solid Earth*, *91*(B9), 9099-9123.

Pe-piper, G., Piper, D., (1989). Spatial and temporal variation in Late Cenozoic back-arc volcanic rocks, Aegean Sea region. Tectonophysics 169, 113–134.

Pe-Piper, G., Piper, D.J.W., Kotopouli, C.N., Panagos, A.G., (1994). Neogene volcanoes of Chios, Greece: the relative importance of subduction and back-arc extension. Geol. Soc. London, Spec. Publ. 81, 213–231. doi:10.1144/gsl.sp.1994.081.01.12

Pe-Piper, G., Piper, D.J.W., Matarangas, D., (2002). Regional implications of geochemistry and style of emplacement of Miocene I-type diorite and granite, Delos, Cyclades, Greece. Lithos 60, 47–66. doi:10.1016/S0024-4937(01)00068-8

Pe-Piper, G., & Piper, D. J. (2006). Unique features of the Cenozoic igneous rocks of Greece. *Geological Society of America Special Papers*, *409*, 259-282.

Pe-Piper, G., Piper, D.J.W., (2007). Neogene backarc volcanism of the Aegean: New insights into the relationship between magmatism and tectonics. Geol. Soc. Am. Spec. Pap. 418, 17–31. doi:10.1130/2007.2418(02)

Pe-Piper, G., Piper, D.J.W., Koukouvelas, I., Dolansky, L.M., Kokkalas, S., (2009). Postorogenic shoshonitic rocks and their origin by melting underplated basalts: The miocene of Limnos, Greece. Bull. Geol. Soc. Am. 121, 39–54. doi:10.1130/B26317.1

Pe-piper, G., Piper, D.J.W., (2013). The effect of changing regional tectonics on an arc volcano: Methana, Greece. J. Volcanol. Geotherm. Res. 260, 146–163. doi:10.1016/j.jvolgeores.2013.05.011

Ranalli, G. (1995). *Rheology of the Earth*. Springer Science & Business Media.

Reilinger, R., McClusky, S., Vernant, P., Lawrence, S., Ergintav, S., Cakmak, R., Ozener, H., Kadirov, F., Guliev, I., Stepanyan, R., Nadariya, M., Hahubia, G., Mahmoud, S., Sakr, K., ArRajehi, A., Paradissis, D., Al-Aydrus, A., Prilepin, M., Guseva, T., Evren, E., Dmitrotsa, A., Filikov, S. V., Gomez, F., Al-Ghazzi, R., Karam, G., (2006). GPS constraints on continental deformation in the Africa-Arabia-Eurasia continental collision zone and implications for the dynamics of plate interactions. J. Geophys. Res. Solid Earth 111. doi:10.1029/2005JB004051

Ring, U., Johnson, C., Hetzel, R., & Gessner, K. (2003). Tectonic denudation of a Late Cretaceous–Tertiary collisional belt: regionally symmetric cooling patterns and their relation to extensional faults in the Anatolide belt of western Turkey. *Geological Magazine*, *140*(04), 421-441.

Salaün, G., Pedersen, H. a., Paul, A., Farra, V., Karabulut, H., Hatzfeld, D., Papazachos, C., Childs, D.M., Pequegnat, C., (2012). High-resolution surface wave tomography beneath the Aegean-Anatolia region: Constraints on upper-mantle structure. Geophys. J. Int. 190, 406–420. doi:10.1111/j.1365-246X.2012.05483.x

Sari, C., Şalk, M., (2006). Sediment thicknesses of the western Anatolia graben structures determined by 2D and 3D analysis using gravity data. J. Asian Earth Sci. 26, 39–48. doi:10.1016/j.jseaes.2004.09.011

Seyitoğlu, G., Scott, B., (1996). The cause of NS extensional tectonics in western Turkey: tectonic escape vs back-arc spreading vs orogenic collapse. J. Geodyn. 22, 145–153.

Sodoudi, F., Kind, R., Hatzfeld, D., Priestley, K., Hanka, W., Wylegalla, K., Stavrakakis, G., Vafidis, a., Harjes, H.-P., Bohnhoff, M., (2006). Lithospheric structure of the Aegean obtained from P and S receiver functions. J. Geophys. Res. 111, B12307. doi:10.1029/2005JB003932

Stein, C. A., & Stein, S. (1992). A model for the global variation in oceanic depth and heat flow with lithospheric age. *Nature*, *359*(6391), 123-129.

Stern, R. J. (2002). Subduction zones. *Reviews of geophysics*, *40*(4).

Şengör, A.M.C., Yilmaz, Y., (1981). Tethyan evolution of Turkey: A plate tectonic approach. Tectonophysics 75, 181–241. doi:10.1016/0040-1951(81)90275-4

van Hinsbergen, D.J.J., Kaymakcı, N., Spakman, W., Torsvik, T.H., (2010). Reconciling the geological history of western Turkey with plate circuits and mantle tomography. Earth Planet. Sci. Lett. 297, 674–686. doi:10.1016/j.epsl.2010.07.024

Uyeda, S., & Kanamori, H. (1979). Back-arc opening and the mode of subduction. *Journal of Geophysical Research: Solid Earth*, *84*(B3), 1049-1061.

Yılmaz, Y., Genç, Ş.C., Gürer, F., Bozcu, M., Yılmaz, K., Karacık, Z., Altunkaynak, Ş., Elmas, A., (2000). When Did the Western Anatolian Grabens Begin to Develop?, Geological Society, London, Special Publications. doi:10.1144/GSL.SP.2000.173.01.1

APPENDIX

Table 6.1 Rersults of all Models

	Physical Properties								C. Thickness	L. Thickness	
	C. Mantle Lithosphere		O. Mantle Lithosphere								
RET-1	Thickness	Coh	Density	Thickness	Con. Vel.	Moho Temp.	Retreat	Max. Subsidence			Streching Factor
RET-2	110	100MPa	3,35	100km	1cm	650	210km	1.6 km	29,0	110,0	1,38
RET-3	110	100MPa	3,35	**110km**	1cm	650	260km	2.7km	27,0	112,5	1,48
RET-4	110	100MPa	3,35	**70km**	1cm	650	180km	1.7km	29,0	110,0	1,38
RET-5	110	100MPa	3,35	**80km**	1cm	650	200km	3,2km	32,0	115,0	1,25
RET-6	110	100MPa	3,35	**90km**	1cm	650	190 km	3,2km	28,0	110,0	1,43

Table-6 (Continued)

RET-7	110	100MPa	**3,29**	100km	1cm	650	30km	2,2km	37,5	145,0	1,07
RET-8	110	100MPa	**3,3**	100km	1cm	650	90km	2,4km	36,0	137,0	1,11
RET-9	110	100MPa	**3,31**	100km	1cm	650	105km	2,7km	34,0	130,0	1,18
RET-10	110	100MPa	**3,32**	100km	1cm	650	150km	2,5km	33,0	120,0	1,21
RET-11	110	100MPa	**3,33**	100km	1cm	650	190km	2,8km	31,0	115,0	1,29
RET-12	110	100MPa	**3,34**	100km	1cm	650	200km	2,8km	30,0	108,0	1,33
RET-13	**50**	100MPa	3,35	100km	1cm	650	350km	4.1km	24,0	55,0	1,67
RET-14	**70**	100MPa	3,35	100km	1cm	650	320km	2.9km	26,0	72,0	1,54
RET-15	**90**	100MPa	3,35	100km	1cm	650	275km	2.4km	26,5	90,0	1,51
RET-16	**40**	100MPa	3,35	**80km**	1cm	650	250km	3,2km	29,0	59,0	1,38
RET-17	**50**	100MPa	3,35	**90km**	1cm	650	260km	2.5km	28,0	64,0	1,43
RET-18	**60**	100MPa	3,35	**100km**	1cm	650	350km	2.6km	24,0	61,0	1,67

Table-6.1 (Continued)

RET-19	**70**	100MPa	3,35	**110km**	1cm	650	360km	3.6km	22,0		62,0	1,82
RET-20	**80**	100MPa	3,35	**120km**	1cm	650	360km	3.6km	22,0		68,0	1,82
RET-21	90	100MPa	3,35	90km	1cm	650	210km	3,2km	29,0		110,0	1,38
RET-22	110	100MPa	3,35	100km	1cm	600	200km	2km	30,0		115,0	1,33
RET-23	110	100MPa	3,35	100km	1cm	700	200km	1.8km	30,0		118,0	1,33
RET-24	110	100MPa	3,35	100km	1cm	750	190km	1.8km	31,0		119,0	1,29
RET-25	110	100MPa	3,35	100km	1cm	800	190km	1.9km	31,0		120,0	1,29
RET-26	110	100MPa	3,35	100km	1cm	850	190km	2km	32,0		121,0	1,25
RET-27	110	100MPa	3,35	100km	1cm	900	190km	1.5km	32,0		122,0	1,25
RET-28	110	100MPa	3,35	100km	1cm	950	170km	1.5km	32,5		123,0	1,23
BOFF-1	50	100MPa	3,35	90km	0cm	650	150km	1km	36,0		80,0	1,11
BOFF-2	110	100MPa	3,35	100km	0cm	650	180km	1.5km		33,50	100	1,19
BOFF-3	90	100MPa	3,35	90km	0cm	650	185km	1.5km		35	102	1,14
BOFF-4	100	100MPa	3,35	100km	0cm	650	90km	0.9km		35	96	1,14

53

6   CURRICULUM VITAE

Name Surname   : **Ziya Mazlum**

Place and Date of Birth   : **Şahinbey/GAZİANTEP 06/09/1989**

E-Mail   : **ziya.mazlum@gmail.com**

EDUCATION   :

• **B.Sc.:** 2014, İstanbul Technical University, Mining Faculty, Geological
    Engineering